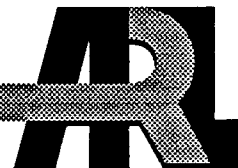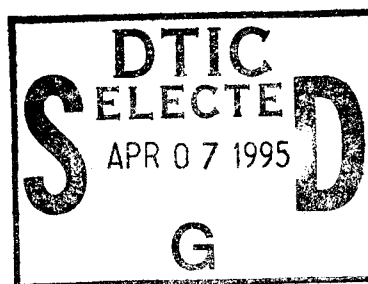# Effects of Hydrostatic Pressure on the Mechanical Behavior of Composite Materials

Christopher P. R. Hoppel
Travis A. Bogetti
U.S. ARMY RESEARCH LABORATORY

John W. Gillespie, Jr.
CENTER FOR COMPOSITE MATERIALS

April 1995

DTIC
SELECTED
APR 0 7 1995
G

19950406 036

DTIC QUALITY INSPECTED 5

**NOTICES**

# REPORT DOCUMENTATION PAGE

*Form Approved*
*OMB No. 0704-0188*

| 1. AGENCY USE ONLY (Leave blank) | 2. REPORT DATE  April 1995 | 3. REPORT TYPE AND DATES COVERED  Final, March 1993–January 1994 |
|---|---|---|

**4. TITLE AND SUBTITLE**

Effects of Hydrostatic Pressure on the Mechanical Behavior of Composite Materials

**5. FUNDING NUMBERS**

PR: 1L162618AH80

**6. AUTHOR(S)**

Christopher P. R. Hoppel, Travis A. Bogetti, and John W. Gillespie, Jr.*

**7. PERFORMING ORGANIZATION NAME(S) AND ADDRESS(ES)**

U.S. Army Research Laboratory
ATTN: AMSRL-WT-PD
Aberdeen Proving Ground, MD 21005-5066

**8. PERFORMING ORGANIZATION REPORT NUMBER**

ARL-TR-727

**9. SPONSORING/MONITORING AGENCY NAME(S) AND ADDRESS(ES)**

**10. SPONSORING/MONITORING AGENCY REPORT NUMBER**

**11. SUPPLEMENTARY NOTES**

**12a. DISTRIBUTION/AVAILABILITY STATEMENT**

Approved for public release; distribution is unlimited.

**12b. DISTRIBUTION CODE**

**13. ABSTRACT** *(Maximum 200 words)*

Hydrostatic pressure can cause significant changes in the mechanical properties of composite materials. A thorough understanding of these effects is essential for the effective design of composite structures for high-pressure applications. In this report, the literature on the effects of hydrostatic pressure on the mechanical behavior of composite materials is reviewed. This includes a general description of the effects of hydrostatic pressure on unreinforced polymers and a detailed critique of the experimental work that has been done on composite materials. The section on composites is divided into three parts: compressive, tensile, and shear testing. For each type of testing, the test materials and techniques and the physical and quantitative results are discussed.

**14. SUBJECT TERMS**

hydrostatic, pressure, triaxial, composite materials, compression, strength

**15. NUMBER OF PAGES**

55

**16. PRICE CODE**

| 17. SECURITY CLASSIFICATION OF REPORT | 18. SECURITY CLASSIFICATION OF THIS PAGE | 19. SECURITY CLASSIFICATION OF ABSTRACT | 20. LIMITATION OF ABSTRACT |
|---|---|---|---|
| UNCLASSIFIED | UNCLASSIFIED | UNCLASSIFIED | UL |

INTENTIONALLY LEFT BLANK.

# ACKNOWLEDGMENTS

| Accesion For | | |
|---|---|---|
| NTIS CRA&I | ☒ | |
| DTIC TAB | ☐ | |
| Unannounced | ☐ | |
| Justification _____ | | |
| By _____ | | |
| Distribution / | | |
| Availability Codes | | |
| Dist | Avail and / or Special | |
| A-1 | | |

Intentionally left blank.

TABLE OF CONTENTS

INTENTIONALLY LEFT BLANK.

LIST OF FIGURES

INTENTIONALLY LEFT BLANK.

LIST OF TABLES

INTENTIONALLY LEFT BLANK.

## 1. INTRODUCTION

The effects of high hydrostatic pressure on materials have been investigated throughout the twentieth century (Vodar and Kieffer 1971). However, early studies concentrated on metallic (Bridgman 1958) and geological materials (Birch 1938). During the last 30 years, it has been shown that hydrostatic pressure has a greater effect on polymer materials than on metals or rocks (Pae and Bhateja 1975). Recent works (Parry and Wronski 1990; Shin and Pae 1992a, 1992b; Sigley, Wronski, and Parry 1992; Sigley, Wronski, and Parry 1991) have shown that the mechanical properties of polymer matrix composites are also strongly affected by hydrostatic pressure. The Army is interested in the use of thick- section-fiber-reinforced-epoxy composites for ballistic applications. Since gun barrels can create a high- pressure environment, effective and efficient design of composite materials for ballistic applications depends on understanding the properties of the composites under hydrostatic pressure.

This report is a summary of the research that has been done on the effects of hydrostatic pressure on polymer matrix composite materials. Since the properties of composites are strongly affected by those of the matrices, section 2 of this report reviews the effects of pressure on unreinforced polymers. Section 3 is a review of the published research on the effects of high pressure on composite materials. This section describes details of the experimental work, effects of the hydrostatic pressure on strengths and stiffnesses, failure modes of the materials, and the quantitative analysis of the results. The significance of the results is then discussed in section 4.

In the experimental work described in this report, the materials were subjected to hydrostatic pressure of up to 1 GPa during testing. The details of the testing facilities will be covered in a separate report. However, one aspect of the testing facilities, the pressure transmitting fluid, was found to affect the test results and will be mentioned here. The pressures were usually transmitted to the material through a fluid such as kerosene or hydraulic oil. While this fluid needs to possess certain mechanical properties (it should be nearly incompressible, so that it stores as little elastic energy as possible, and it should also be lubricating to prolong the life of the pressurizing pump), the major concern in analysis of previous results is how the fluid interacts with the test materials. In tests on geological materials the test specimens are usually sealed in a rubber or copper jacket to prevent interaction with the confining fluid (Brown 1981; Heard 1963). In most of the tests on unreinforced polymers reviewed in this study, the polymers were not protected from the pressure-transmitting fluid. Laka and Dzenis (1967) and Sauer (1977) have reported that the pressure medium has a strong effect on the mechanical properties of brittle polymers such

1

as Plexiglass, but little effect on ductile polymers such as polyethylene. In the tests on the composite materials, most of the specimens were protected from the confining fluid by a rubber coating. Of the tests that were conducted without a protective coating, only one study (Sigley, Wronski, and Parry 1992) reported any effects of the confining fluid on the test materials; these results were subsequently omitted from this review.

## 2. EFFECTS OF PRESSURE ON THE MECHANICAL PROPERTIES OF UNREINFORCED POLYMERS

Pae and Bhateja (1975) gave a very detailed review of the literature up to 1975 of the mechanical behavior of polymers under pressure. The authors discussed all of the research to date on each polymer that had been studied. The reader is referred to this article and more recent studies (Sauer 1977) for a thorough review of the effects of hydrostatic pressure on polymers. This section of the report will highlight some of the important effects of hydrostatic pressure on polymers, and it will analyze those effects in terms of the physical changes in the materials.

2.1 <u>Elastic Modulus</u>. In general, the elastic modulus of unreinforced polymers increases with increasing hydrostatic pressure in tension, compression, and shear in either a linear or piece-wise linear manner. Figure 1 shows the ratio of the elastic modulus under hydrostatic pressure to the modulus at atmospheric pressure for several crystalline polymers. Figure 2 shows the same information for several amorphous polymers. In general, the pressure dependence of the modulus is greater for materials that have low moduli at atmospheric pressure. The pressure dependence is then greater for crystalline polymers that have a glass transition below the test temperature than for amorphous polymers that are glassy at the test temperature (Pae and Bhateja 1975).

According to Pae (Pae and Bhateja 1975), one of the main reasons for the increase in the elastic modulus with increasing pressure is the effects of finite deformations on the polymer. In classical theory of elasticity, strains are referred to as infinitesimal if the squares and products of the strains are so small that they can be neglected. When the strains are finite or large enough that their squares and products can no longer be neglected, classical theory of elasticity no longer holds, and the finite deformation theory of elasticity developed by Murnaghan (1937, 1951) is used. In experimental work on the effects of high pressure on the mechanical behavior of polymers, the pressures used can be much higher than the applied axial loads, and often on the order of the elastic moduli of the materials (Pae and Sauer 1970). At these

2
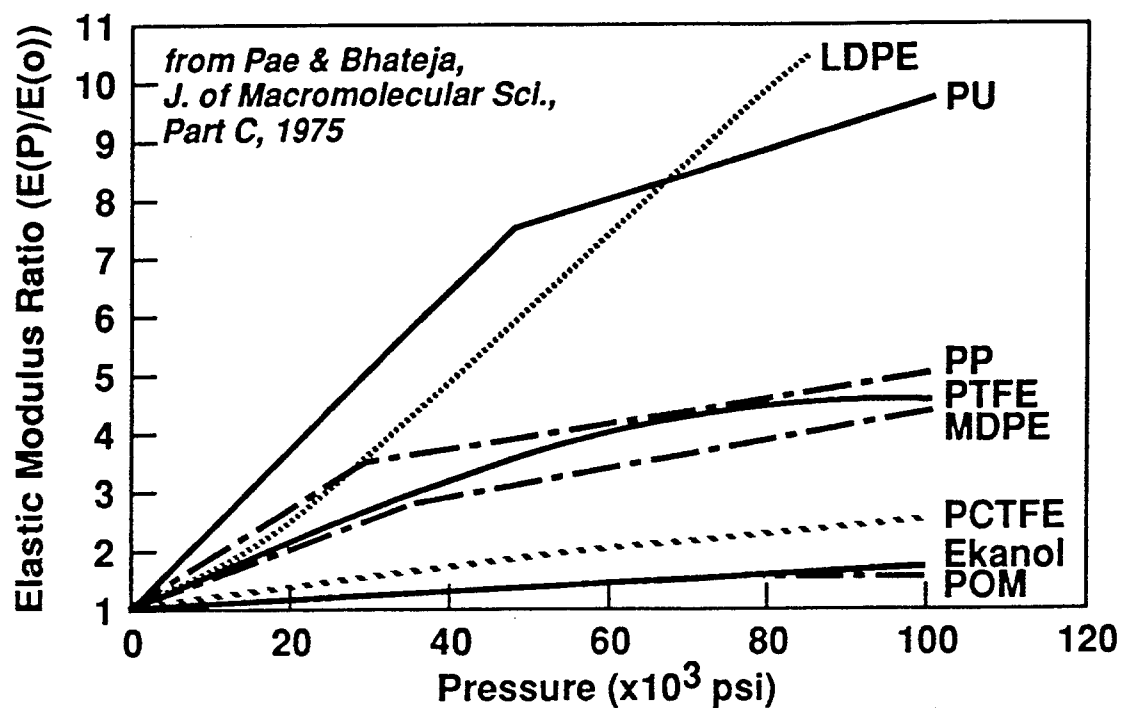
Figure 1. Elastic modulus ratio vs. pressure for various crystalline polymers.
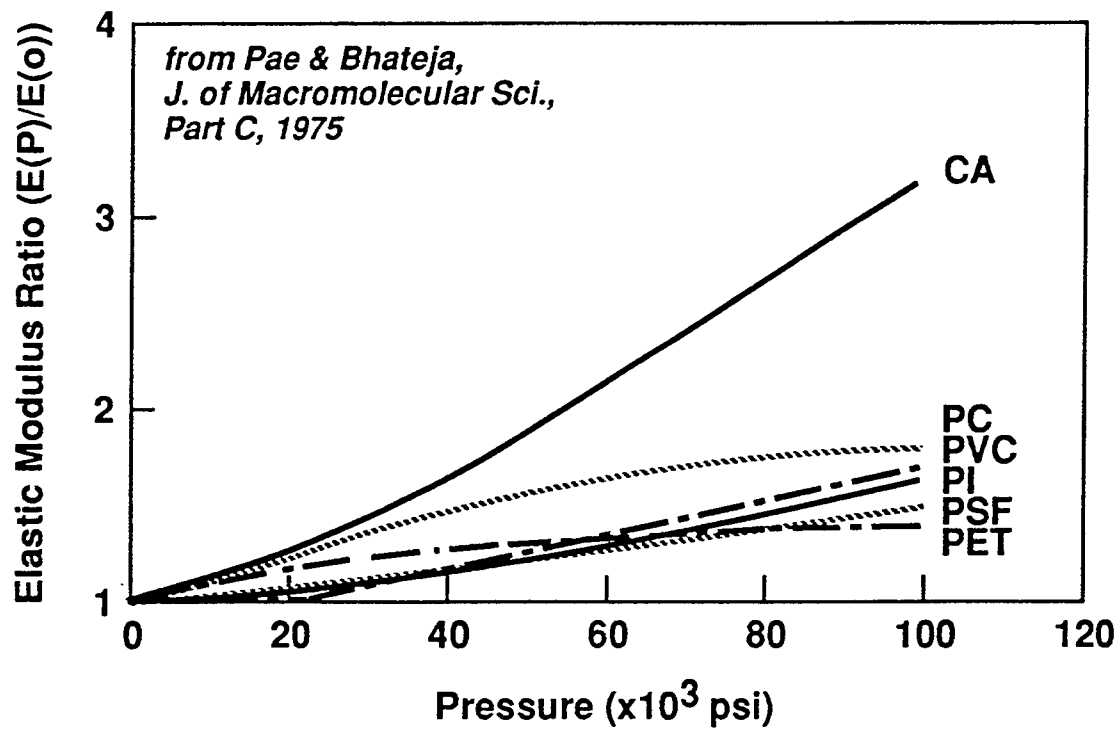


Figure 2. Elastic modulus ratio vs. pressure for various amorphous polymers.

pressures the elastic modulus is no longer constant but is a function of the applied pressure (Pae and Bhateja 1975). Birch (1938) proposed that at high pressures the modulus is a function of the pressure and the Poisson's ratio as shown in equation 1:

$$E = E(0) + (P * 2(5 - 4\upsilon)(1 - \upsilon)) , \tag{1}$$

where $E(0)$ is the elastic modulus at atmospheric pressure, P is the applied hydrostatic pressure, and $\upsilon$ is the Poisson's ratio at atmospheric pressure. Equation 1 can be normalized with respect to the initial modulus as follows:

$$\frac{E}{E(0)} = 1 + \frac{P}{E(0)} 2 (5 - 4\upsilon)(1 - \upsilon) . \tag{2}$$

Equations 1 and 2 predict that the elastic modulus of a material will increase proportionally to the hydrostatic pressure with a slope of $2(5 - 4\upsilon)(1 - \upsilon)$. However, the effects of this are much more significant in materials with initially low moduli (such as polymers) than in materials with high moduli (such as metals and ceramics). For example, if polypropylene (PP) [$E(0)$ = 1.45 GPa, $\upsilon$ = 0.32] and iron [$E(0)$ = 211.4 GPa, $\upsilon$ = 0.293] were tested under 300-MPa hydrostatic pressure, the modulus of the PP would be expected to increase 105% and the modulus of the iron would only increase 0.8%. Thus, the effects of the pressure on the modulus of polymers is much more significant than the effects on the moduli of stiffer materials.

The shear modulus has also been shown to be a function of the applied hydrostatic pressure as described by equation 3 (Birch 1938; Sauer 1977):

$$G(P) = G(0) + \frac{3(3 - 4\upsilon)}{2(1 + \upsilon)} P . \tag{3}$$

Like the equation for the elastic modulus (equation 1), the equation for the shear modulus is a function of the initial shear modulus. Materials that have initially low moduli will show a much stronger pressure dependence than materials with initially high moduli.

4

Pae and Bhateja (1975) reported the measured slopes of the elastic modulus vs. hydrostatic pressure curves for several polymers and the slopes that were calculated from the Birch equation (equation 1), and these values are given in Table 1. For the materials listed in Table 1, the Birch equation predicts the pressure dependence of the elastic modulus fairly accurately. This is significant because all of the constants in the Birch equation can be found from tests at atmospheric pressure. However, Matsushige, Radcliffe, and Baer (1975) have shown that for polymethyl methacrylate (PMMA), the pressure vs. modulus curve is nonlinear at high pressures. This led Sauer (1977) to suggest that the Poisson's ratio may be an increasing function of pressure, so that the Birch equation is not accurate at high pressures.

Table 1. Predicted and Experimental Slope of the Elastic Modulus vs. Pressure Curve

| Material | Elastic Modulus (GPa) | Poisson's Ratio | Slope Predicted by the Birch Equation | Observed Slope | Reference |
|---|---|---|---|---|---|
| PTFE | 1.52 | 0.45 | 3.5 | 3.3 | Pae and Bhateja 1975 |
| PCTFE | 1.17 | 0.44 | 3.6 | 3.0 | Silano and Pae 1972 |
| PE | — | 0.34 | 4.8 | 4.1 | Silano, Bhateja, and Pae 1974 |
| PP | 1.45 | 0.32 | 5.1 | 4.1 | Silano, Bhateja, and Pae 1974 |
| PC | 2.45 | 0.38 | 4.3 | 4.1 | Pae and Bhateja 1975 |
| CA | 1.52 | 0.33 | 4.9 | 5.1 | Pae and Bhateja 1975 |
| PI | 2.09 | 0.41 | 4.0 | 3.0 | Silano, Bhateja, and Pae 1974 |
| PVC | 2.26 | 0.40 | 4.0 | 3.2 | Silano, Bhateja, and Pae 1974 |

While the Birch equation can be used to predict the initial linear response of the elastic modulus due to hydrostatic pressure, high hydrostatic pressure can also cause the glass transition and subglass transitions in a polymer to shift to higher temperatures, which causes the modulus to increase at a different rate. Paterson (1964) observed that the glass transition of rubber increased by 80° C with 510 MPa

(74 ksi) of applied hydrostatic pressure. This caused the elastic modulus to increase by over two orders of magnitude.

Hydrostatic pressure can also raise the temperature of secondary glass transitions. In torsion tests on unreinforced epoxy samples, Shin and Pae (1992a) reported that the slope of the modulus vs. pressure curve for epoxy changed at 200 MPa (29 ksi) due to a subglass transition in the epoxy as shown in Figure 3. In fracture toughness tests on polyethylene, Truss, Duckett, and Ward (1984) reported that the gamma transition for polyethylene normally occurs at -100° C. Hydrostatic pressure raised this transition at a rate of ~15° C per 100 MPa (14.5 ksi) of applied pressure so that at 800 MPa (116 ksi), the gamma transition occurred at room temperature (20° C).
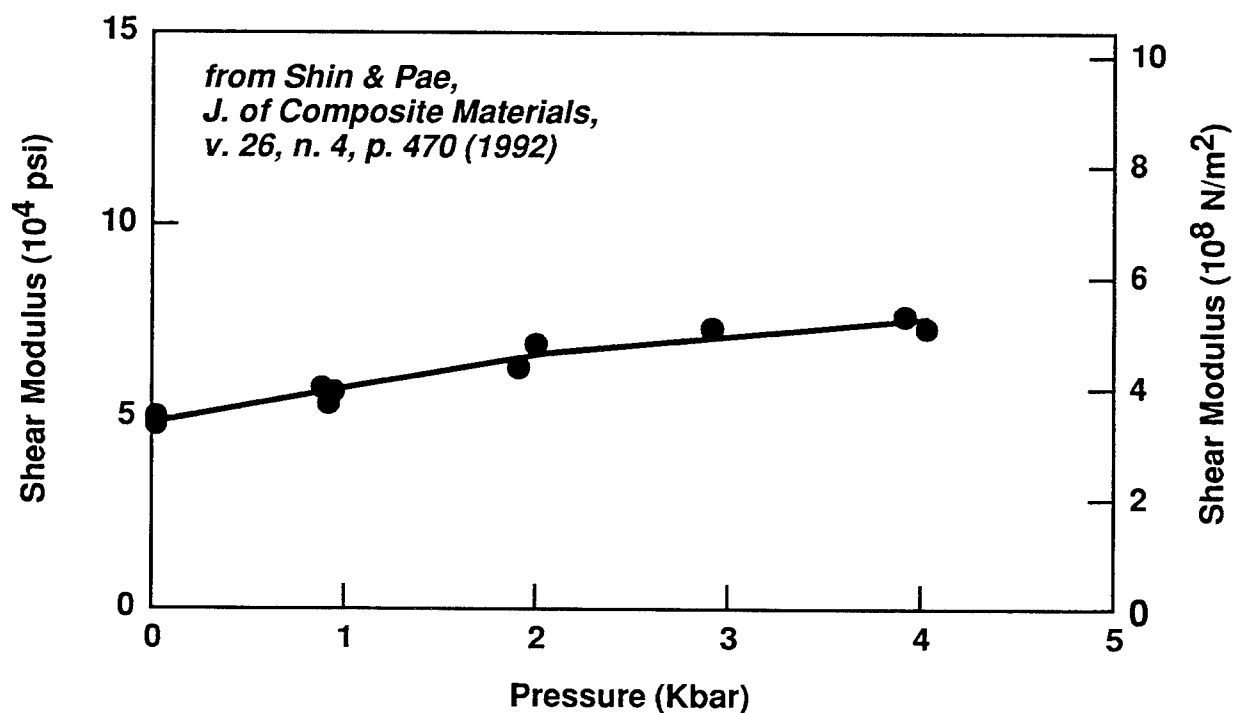
Figure 3. Torsional shear modulus vs. pressure for tubular samples of epoxy matrix.

The effects of pressure can also vary depending on the crystallinity of the polymer. For example, in tests on low-density and medium-density polyethylene (LDPE and MDPE) (Silano, Bhateja, and Pae 1974; Mears, Pae, and Sauer 1969), both materials showed increasing stiffness and strength with increasing pressure; however, the stiffness and strength increased at a much higher rate for the LDPE due to the higher compressibility of this material. The modulus vs. pressure curves for both materials showed a nonlinear point at 240 MPa (35 ksi). This pressure corresponded to the β-transition for polyethylene.

2.2 Yield Strength. The yield strength of polymers also increases with applied hydrostatic pressure; however, the pressure dependence of the yield strength usually differs from that of the modulus. In tensile and compression tests on polyvinyl chloride and cellulose acetate at pressures from atmospheric to 690 MPa (100 ksi), Pae and Sauer (1970) found that the yield strength increased linearly with increasing pressure for both materials in tension and compression. However, the relationship between the modulus and pressure was bilinear with a pressure-induced transition at 138 MPa (20 ksi). Sauer (1977) later suggested that in semicrystalline polymers, the modulus is more strongly affected by the properties of the amorphous phase, and the yield stress is more strongly dependent on the crystalline phase. When a material undergoes a pressure-induced glass transition, the amorphous phase and the modulus of the material show a greater change. Therefore, while the modulus vs. pressure curves are often bilinear for polymers, the yield stress vs. pressure curves are usually linear (Sauer 1977).

Christiansen, Baer, and Radcliffe (1971) found that for polycarbonate the modulus increased by 40% between atmospheric pressure and 800 MPa (116 ksi); however, over the same pressure range the yield stress increased 240%. This indicated that the mechanisms controlling the elastic modulus were not the same as those controlling plastic flow. The authors compared the change in yield stress to the change in the amount of free volume in the material. They found that the yield stress increases at a higher rate for a change in volume caused by a decrease in temperature than for a change in volume caused by an increase in pressure (Christiansen, Baer, and Radcliffe 1971). This could be caused by the additional effects caused by the temperature change, such as a decrease in polymer chain mobility. The yield strengths of several polymers and their dependencies on hydrostatic pressure are given in Table 2.

Several theories have been proposed to explain the dependence of the yield stress on the 3-D stress state. The Mohr-Coulomb theory (Pae and Bhateja 1975; Sauer 1977; Bhateja and Pae 1972) and the modified von Mises theory (Pae and Bhateja 1975; Sauer 1977; Sternstein and Ongchin 1969) are given in equations 4 and 5. Both of the equations predict that the yield stress in any one direction will increase linearly with increasing hydrostatic pressure. The Mohr-Coulomb theory predicts that yielding will occur when a combination of the normal and shear stresses reach a critical value; the modified von Mises equation assumes that yielding will occur when the octahedral shear stress ($\tau_{oct}$) reaches a value which is a linear function of the mean stress ($\sigma_m$) (Sauer 1977).

$$\tau + \mu' \, \sigma_n = \tau_0 , \tag{4}$$

$$\tau_{oct} = \tau_s - \mu \sigma_m . \tag{5}$$

7

Table 2. Dependence of Unreinforced Polymer Yield Strengths as a Function of Pressure

| Material | Type of Test | Reference | Atmospheric Yield Strength (MPa) | Slope |
|---|---|---|---|---|
| POM | compression | Pae 1977 | 77.2 | 0.14 |
| POM | tension | Truss, Duckett, and Ward 1984 | 73.1 | 0.13 |
| POM | shear | Pae 1977 | 50.3 | 0.07 |
| PP | compression | Pae 1977 | 50.3 | 0.07 |
| PP | tension | Truss, Duckett, and Ward 1984 | 37.2 | 0.21 |
| PP | compression | Pae 1977 | 24.1 | 0.12 |
| PE | tension | Pae and Sauer 1970 | 26.2 | 0.094 |
| PTFE | tension | Pae and Sauer 1970 | 9.0 | 0.080 |
| PTFE | compression | Pae and Sauer 1970 | 14.1 | 0.094 |
| PC | tension | Pae and Sauer 1970 | 84.1 | 0.083 |
| PVC | tension | Pae and Sauer 1970 | 62.1 | 0.135 |
| PVC | compression | Pae and Sauer 1970 | 75.9 | 0.202 |
| CA | tension | Pae and Sauer 1970 | 41.4 | 0.196 |
| CA | compression | Pae and Sauer 1970 | 48.3 | 0.210 |
| Beetle 811 polyester | compression | Sigley, Wronski, and Parry 1992 | 80.0 | 0.160 |
| Stypol 40–1077 polyester | compression | Sigley, Wronski, and Parry 1992 | 120.0 | 0.420 |
| epoxy | compression | Wronski and Pick 1977 | 88.0 | 0.707 |

Cadell, Raghava, and Atkins (1974) and Pae and Bhateja (1975) proposed the following theory for yielding:

$$(\sigma_1 - \sigma_2)^2 + (\sigma_2 - \sigma_3)^2 + (\sigma_3 - \sigma_1)^2 + 2(C - T)(\sigma_1 + \sigma_2 + \sigma_3) = 2CT, \tag{6}$$

where C and T are the absolute values of the compressive and tensile yield strengths at atmospheric pressure. This yielding theory is significant because it accounts for the differences in the compressive and tensile yield strengths in most polymers. For example, the ratio of the compressive to tensile yield strength for polyoxymethylene (POM) is 1.16. This theory predicts that both the compressive and tensile yield strengths will increase linearly with increasing pressure. For materials which have equal tensile and compressive yield strengths, equation 6 becomes the pressure-independent von Mises criterion (Caddell, Raghava, and Atkins 1974).

Hu and Pae (1963) proposed a yield theory for materials subject to hydrostatic pressure based on the stress invariants:

$$\sqrt{J_2'} = \sum_{n=0}^{\infty} \alpha_n J_1^n , \tag{7}$$

where $J_1 = \sigma_{kk}$ (the first stress invariant), $J_2' = \frac{1}{2}\sigma_{ij},\sigma_{ij}$ , (the second stress invariant), and $\alpha_n$ are material constants. When $n = 0$, equation 7 is the von Mises yield criterion. When $n = 1$, equation 7 can be written as follows:

$$\sqrt{J_2}' = \alpha_0 + \alpha_1 J_1 . \tag{8}$$

Equation 8 predicts that the yield stress will have the following linear dependence on hydrostatic pressure.

$$\sigma_{yield} = (\frac{\sqrt{3}}{1 \pm |\alpha_1|\sqrt{3}})(\alpha_0 + 3|\alpha_1|P) , \tag{9}$$

where the plus sign refers to the tensile case and the minus sign refers to the compressive (Pae and Bhateja 1975; Silano, Bhateja, and Pae 1974). It is important to note that equation 7 can be rewritten in the form of any of equations 4–6.

Pae (1977) evaluated the yielding of POM and PP under hydrostatic pressure combined with uniaxial tension and compression and pure shear loading, and found that each yield stress showed a different pressure dependence. All three yield strengths increased with increasing hydrostatic pressure for both of the experimental materials. For POM, the shear yield strength increased at a rate of 0.068 times the hydrostatic pressure. The tensile yield strength increased at a rate of 0.12 times the hydrostatic pressure. The compressive yield strength increased at a rate of 0.13 times the hydrostatic pressure. The 3-D yield surfaces are shown in Figure 4 for POM and in Figure 5 for PP. Part *a* for each figure shows how the tensile, shear, and compressive yield stresses varied under hydrostatic pressure. Part *b* of each figure shows the intersection of the yield surface at atmospheric pressure with the π-plane, which is a hyperplane with a normal in the direction of the hydrostatic axis $(\frac{1}{\sqrt{3}}, \frac{1}{\sqrt{3}}, \frac{1}{\sqrt{3}})$ . Part *c* of each figure shows the 2-D projection of the yield surfaces at zero pressure. Pae (1977) concluded that equation 7 could be used to predict the yield behavior of both materials, with n = 1 for POM and with n = 2 for PP.

Wronski and Pick (1977) evaluated the yield criteria for two epoxy resins. Figure 6 shows the 2-D projection of the yield strength data for tensile and compressive tests under hydrostatic pressure, and Figure 7 shows the 2-D projection of the yield strength data for shear tests under hydrostatic pressure. Four curve fits are given in each of the figures. The cone fit corresponds to equation 5 (the modified von Mises theory), the paraboloid fit corresponds to equation 6 (the theory proposed by Cadell), the two-parameter pyramid corresponds to equation 4 (the Mohr-Coulomb theory), and the three-parameter pyramid is a modified version of the Mohr-Coulomb theory. The authors reported that the best fit was either the two-parameter or three-parameter pyramid model (Wronski and Pick 1977).

2.3 <u>Fracture Properties</u>. The fracture properties of the polymers that were studied varied depending on the failure mechanisms in the materials and the test conditions. The ultimate tensile strengths (maximum stress) of the polymers always increased with increasing hydrostatic pressure. Sauer (1977) attributed this to the effects of pressure on molecular mobility. At high pressures the molecular chains are forced closer together, decreasing mobility, so that higher stresses are necessary to produce a given strain (Sauer 1977). The ultimate strength is often affected by pressure in the same manner as the yield strength. In PP (Sauer 1977; Yoon, Pae, and Sauer 1976) and PTFE (Sauer 1977), the fracture strength increased proportionally to the yield strength. However, in other polymers the effects of pressure on the fracture strength depended on the dominant failure mechanisms. Pae and Bhateja (1975) and Sauer, Pae,

$$\left(\frac{1}{\sqrt{3}}, \frac{1}{\sqrt{3}}, \frac{1}{\sqrt{3}}\right)$$

*from Pae, J. of Mat. Sci.,
v. 12, p. 1212 (1977)*

◦ Experimental Data

$\sigma_2/\sigma_{ot}$

$\sigma_3/\sigma_{ot}$

Von Mises
Yield
Condition

$\sigma_1/\sigma_{ot}$

π Plane

Tension Under
Hydrostatic
Pressure

$\sigma_3/\sigma_{ot}$   $\sigma_2/\sigma_{ot}$

Von Mises

Tresca

(b)

$\sigma_1/\sigma_{ot}$

Shear
Under
Hydrostatic
Pressure

$\sigma_2/\sigma_{ot}$   (c)

$\sigma_1/\sigma_{ot}$

Tresca

Compression
Under Hydrostatic
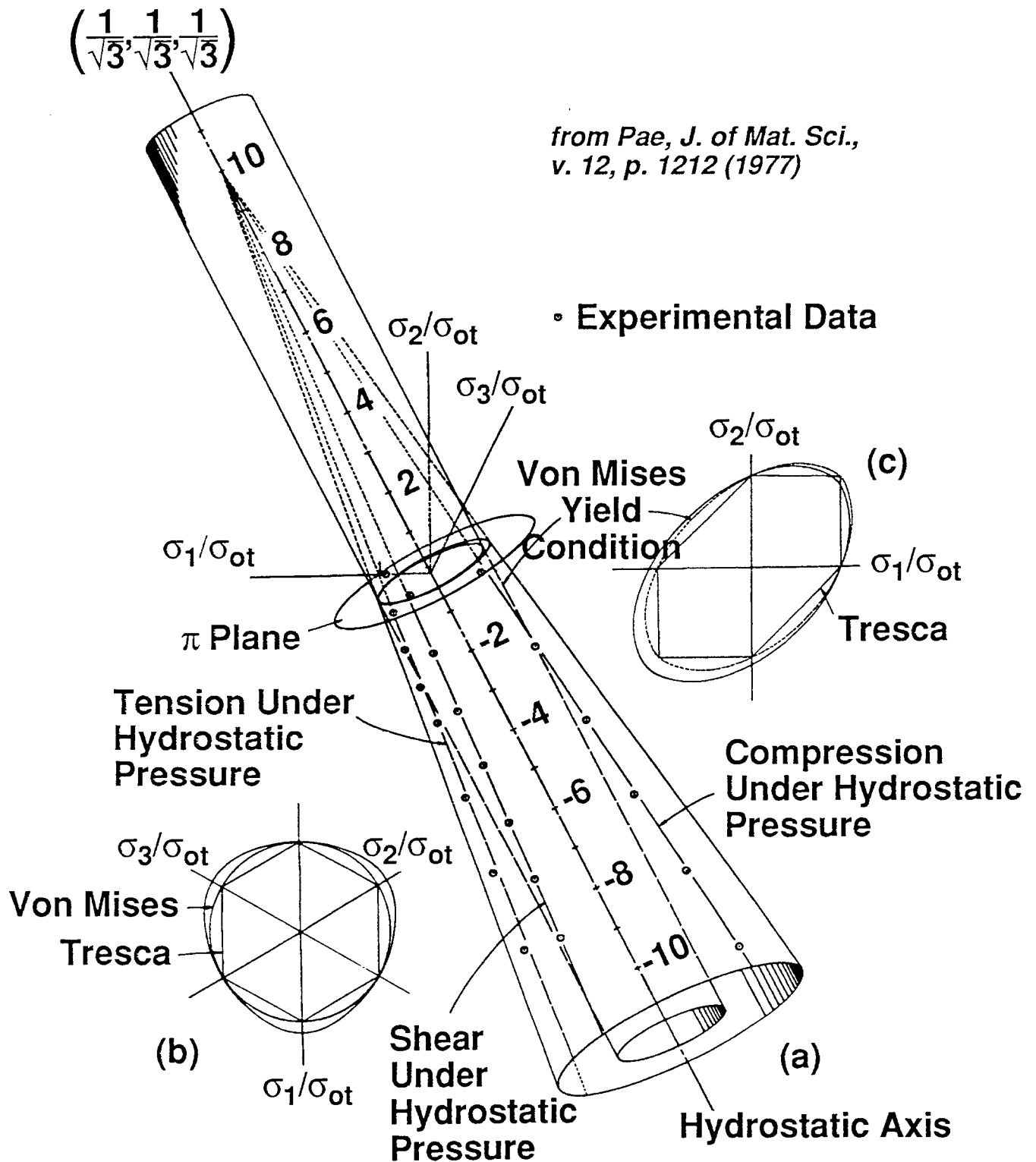Pressure

(a)

Hydrostatic Axis

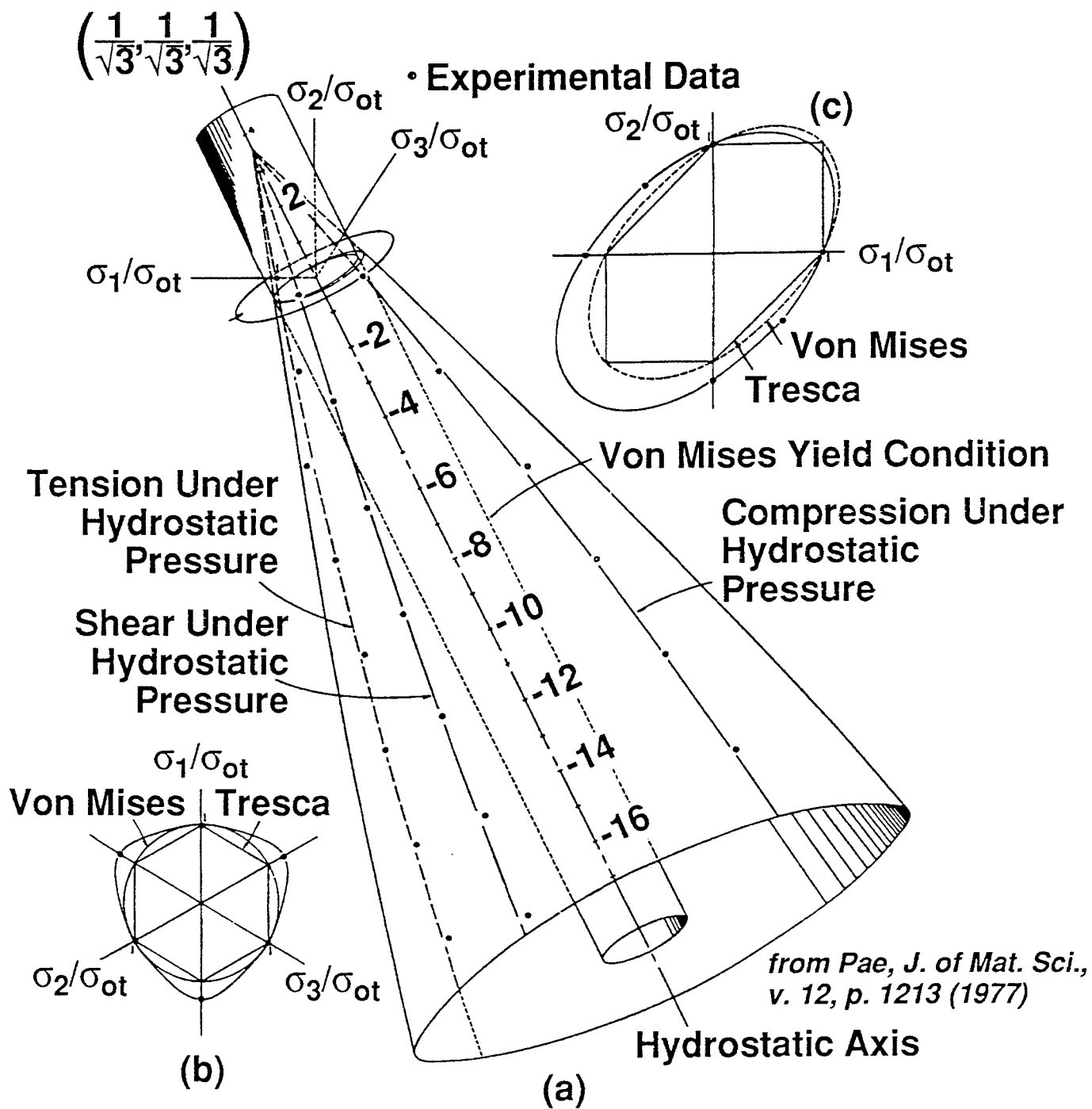Figure 4.  Three-dimensional yield surface of POM.

11
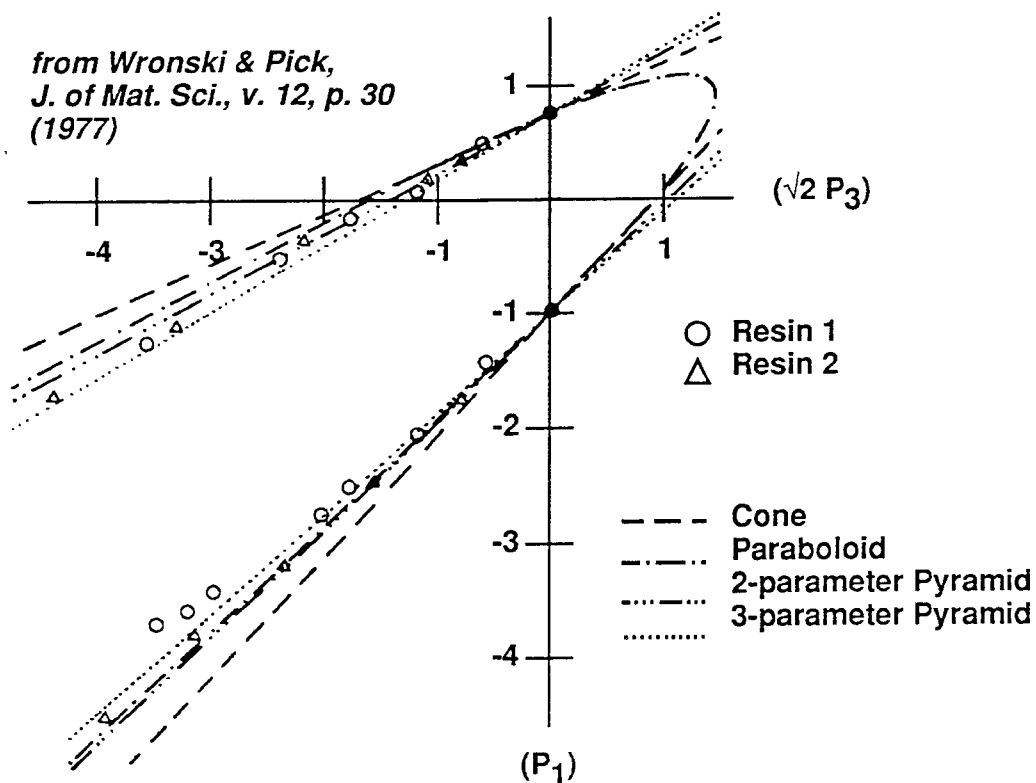
Figure 5. Three-dimensional yield surface of PP.

Figure 6. Yield strength data for tensile and compressive tests of an epoxy resin under superposed hydrostatic pressure.
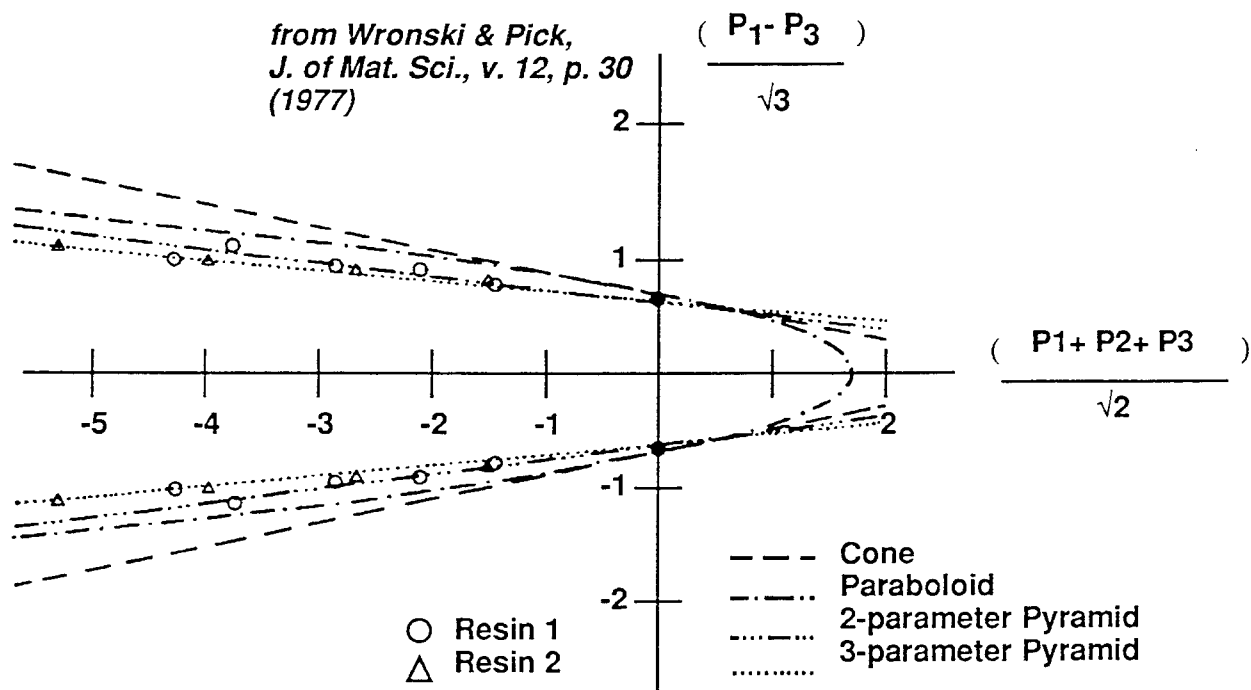


Figure 7. Yield strength data for shear tests of an epoxy resin under superposed hydrostatic pressure.

and Bhateja (1975) found that the compressive fracture strength of poly-p-oxybenzoyl (Ekonol) increased at a high rate between pressures of atmospheric, and about 300 MPa (44 ksi) when the failure was primarily shear. At higher pressures the failure mode changed to axial cleavage, and the strength did not increase at as high of a rate.

While the elastic modulus yield strength and fracture strength of most polymers increase with increasing hydrostatic pressure, the effects of pressure on the fracture strain vary between polymers, depending on the deformation mechanisms and testing environment. In general, high pressure suppresses deformation mechanisms that cause an increase in volume in the polymer, and does not affect mechanisms which are constant volume processes.

Crazing, which is a dominate deformation mechanism in many polymers at atmospheric pressure, is almost completely eliminated under high pressure. Gol'dman, Mesh, and Korchagin (1985) used small angle x-ray scattering (SAXRS) to analyze the density of deformed regions in high-density polyethylene tested at pressures between atmospheric and 200 MPa (29 ksi). At atmospheric pressure the material deformed through craze formation and the fracture surface showed a great deal of stress whitening. The density of the deformed material was approximately half of the undeformed polymer. When the material was tested under hydrostatic pressure, the crazing and stress whitening were eliminated at pressures above 20 MPa (2.9 ksi) and the density of the material at the fracture surface was almost equal to the undeformed polymer. The density of the deformed material did not vary with test pressure at pressures greater than 20 MPa (Gol'dman, Mesh, and Korchagin).

High pressure can also inhibit the formation and growth of cracks in polymers. Sauer (1977) reported that the surface energy g, associated with fracture surfaces, increases with increasing pressure. This increases the amount of work needed to cause a crack to form and grow in the material. When brittle crack growth is inhibited, the material can deform plasmically prior to failure. For example, POM is brittle at atmospheric pressure because of the presence of flaws; however, at high pressures the flaws do not grow and the material deforms plasmically and shows large increases in strain to failure (Silano, Bhateja, and Pae 1974).

While the pressure can suppress crack initiation, it also raises the yield stress and inhibits local yielding in the polymer. Since local yielding is often desirable because it slows crack growth, the suppression of yielding can make the material more brittle. When cellulose acetate, a ductile polymer at

14

atmospheric pressure, was tested under hydrostatic pressure it became much more brittle, and the strain to failure decreased with increasing pressure (Pae and Sauer 1970).

Sweeney, Duckett, and Ward evaluated the effects of hydrostatic pressure on crack growth by testing the fracture toughness of notched tension (1988), and notched torsion (1986; Sweeney et al. 1985) specimens of oriented polyethylene at high hydrostatic pressure. The authors found that pressures of 400 MPa (58 ksi) raised the yield strength of the materials so that there was no plastic zone in front of the growing crack tip. Therefore, the fracture toughness was much lower than at atmospheric pressure. However, at higher pressures (between 400 MPa and 1 GPa), the fracture toughness did not appear to vary with the hydrostatic pressure. In a study on the effects of pressure on notched polyvinyl chloride (PVC) (Sweeney, Duckett, and Ward 1985), the authors found that while the PVC showed extensive stress whitening at atmospheric pressure, plastic deformation was completely eliminated at hydrostatic pressures of 250 MPa (36 ksi). The fracture toughness of the PVC was much lower at 250 MPa (36 ksi) than at atmospheric pressure; however, at higher pressures (between 250 MPa and 1 GPa), the fracture toughness increased with increasing pressure.

Since crazing, local yielding, and cracking all interact during the plastic deformation of most polymers and hydrostatic pressure affects each mechanism in a different manner, the pressure can have several effects on the strain to failure for single polymers. PVC (Pae and Sauer 1970), polyurethane (Silano, Bhateja, and Pae 1974), and polystyrene (Pae and Bhateja 1975) all display a ductile-brittle-ductile transition: they are ductile at atmospheric pressure, behave in a brittle manner at higher pressures, then become more ductile at even higher pressures. Biglione, Baer, and Radcliffe (1969) evaluated this transition by studying the tensile behavior of unreinforced polystyrene, high-impact polystyrene (HIPS), and acrylonitrile-butadiene-styrene (ABS) under hydrostatic pressure. They found that at atmospheric pressure all of these materials deform by forming crazes which can blunt cracks growing from flaws. At higher pressures the crazes were suppressed, and the failure was brittle from the small cracks and inherent flaws in the polymers. At higher pressures the crack growth was slowed by the hydrostatic pressure, and the materials were able to deform to a greater extent than under atmospheric conditions (Biglione, Baer, and Radcliffe 1969).

15

2.4 Effects of Polymer Properties on Composite Properties. Sections 2.1 through 2.3 have shown that the properties of polymers show considerable changes when they are tested under hydrostatic pressure. Figure 8 shows the effect of hydrostatic pressure on the compressive stress-strain behavior of an epoxy resin, which is used extensively as a matrix material in high-performance composites. Notice that the modulus, yield strength, and fracture strength all increase with increasing hydrostatic pressure.
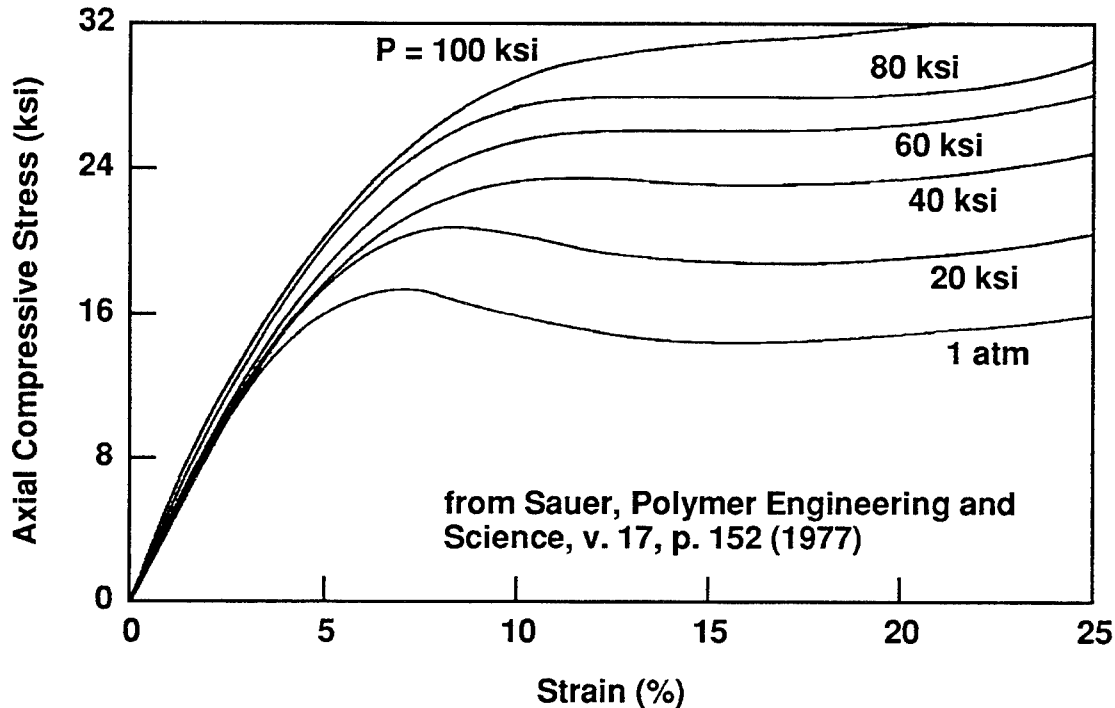


Figure 8. Effect of pressure on the compressive stress-strain behavior of an epoxy resin.

In a fiber-reinforced-epoxy composite, the modulus of the fibers is usually much higher than the modulus of the matrix and the fibers show very little pressure dependence. The rule of mixtures (equation 10) predicts that the changes in the matrix modulus will have little effect on the composite modulus (Agarwal and Broutman 1980). However, as will be shown in section 3, the strength and fracture properties of composite materials show significant pressure-induced effects. These effects are due to the effects of the matrix materials on the micromechanics of fracture in the composite materials. The increased modulus and yield strength of the polymers limits localized plastic deformation in the composite materials, making them more resistant to localized fiber buckling and kinking in compression. However, the increased yield strength also decreases the toughness of the matrix material, decreasing the amount of crack blunting that can occur in the composite materials.

$$E_c = E_f V_f + E_m V_m \tag{10}$$

## 3. EFFECTS OF HYDROSTATIC PRESSURE ON THE MECHANICAL BEHAVIOR OF COMPOSITE MATERIALS

3.1 Compression of Composite Materials. The first study of the effects of hydrostatic pressure on composite materials was conducted by Weaver and Williams (1975), who investigated the compression response of carbon-epoxy composites under hydrostatic pressure. The composites consisted of Modmur Type II carbon fibers (36% volume fraction) in an Epikote 828 epoxy resin. The material was pultruded into 5-mm-diameter rods, which were subsequently cut into 10-mm unidirectional test specimens. The authors reported that the fibers were not well aligned or uniformly distributed, so that the strengths of the materials were less than those of well-aligned specimens.

The specimens were tested in an apparatus designed by Heard (1963), which was capable of applying hydrostatic pressures of up to 500 MPa (72.5 ksi). Ethyl alcohol was used as the confining fluid. To protect the specimens from the confining fluid they were sealed in a rubber sleeve and surrounded by an annealed copper jacket (0.25 mm thick). The pressure to deform the rubber and copper jackets was considered small compared to the load carried by the test specimen. The specimens were end loaded in uniaxial fiber compression at a rate of 0.125 mm/min while exposed to the hydrostatic pressure of the confining fluid. The axial load on the specimens was measured through an internal load cell, and the deformation was measured from the displacement of the deforming piston (Weaver and Williams 1975).

Stress vs. strain curves for the composites under hydrostatic pressure are shown in Figure 9. The behavior of the composites appears to be fiber dominated at all pressures, and no plastic deformation is observed in the specimens. The elastic moduli do not appear to change with pressure, but strength and the strain to failure increase with increasing pressure. At atmospheric pressure the average failure stress is 511 MPa (74 ksi) and the strain to failure is about 2%. At 500-MPa (72.5 ksi) hydrostatic pressure, the failure strain is approximately 4% and the compressive strength is approximately 1,100 MPa (160 ksi). The materials exhibited a bilinear pressure dependence. For pressures up to 100 MPa (14.5 ksi), the uniaxial compressive strength increases at a rate of 3.2 times the applied hydrostatic pressure. For pressures between 100 MPa and 500 MPa (72.5 ksi), the compressive strength increases at a rate of 1.0 times the applied pressure (Weaver and Williams 1975).

The observed failure modes for the composites changed with increasing pressure. At atmospheric pressure the specimens generally failed by longitudinal splitting and brooming at the ends. At higher
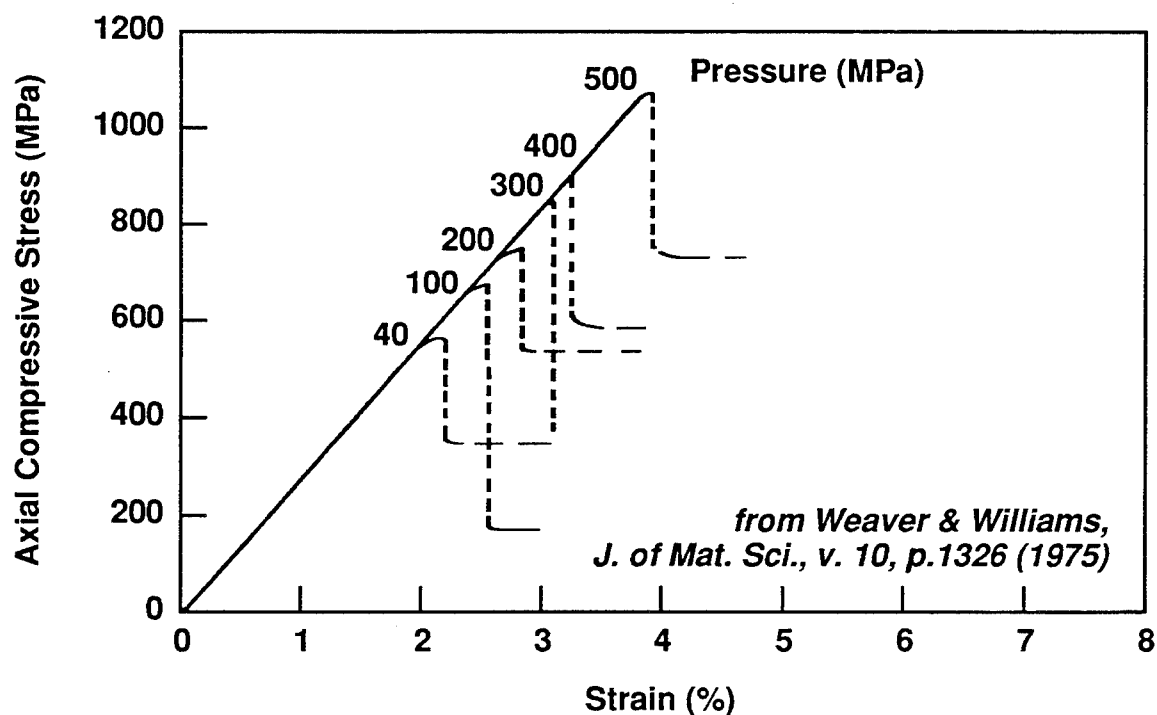
Figure 9. Stress-strain curves for a carbon-fiber-reinforced-epoxy composite deformed in compression under hydrostatic pressure.

pressures the splitting was generally contained and the deformation occurred in localized bands across the specimens. The deformed regions were due to fiber kinking and transverse cracking. In the kinked regions the fibers fractured in several places due to the bending. The length of the broken fibers decreased with increasing pressure. At atmospheric pressure the average fiber segment was 0.07 mm in length; at 500-MPa (72.5 ksi) hydrostatic pressure the average fiber segment was 0.02 mm in length (Weaver and Williams 1975).

The authors reported that while they do not believe that the fiber properties changed with increasing pressure, the elastic modulus and the yield strength of the epoxy both increased over 30% between atmospheric pressure, and 500 MPa of hydrostatic pressure. This indicated that the change of strength in the composite may have been due to the effect of the stiffer matrix on fiber kinking (Weaver and Williams 1975).

Wronski, Parry, and Sigley at the University of Bradford in West Yorkshire England studied the effects of hydrostatic pressure on the tensile, compressive, and shear properties of glass- and carbon-fiber-reinforced composites. Like Weaver and Williams, all of the testing by Wronski et al. was conducted on

pultruded unidirectional composite specimens so the fibers were not always aligned well. The specimens were tested in a pressure cell which was capable of applying pressures up to 300 MPa (43.5 ksi), using Plexol (a synthetic diester) as the pressurizing fluid. Loads were applied to the specimens using a universal testing machine, and were measured with a load cell located outside of the pressure cell, so the final results had to be corrected for the frictional forces at the pressure cell seals. To do this, the authors assumed that friction was constant throughout the hydrostatic region investigated (Parry and Wronski 1985).

In their first study, Parry and Wronski (1979, 1981) investigated the flexure properties of beams made of epoxy reinforced with 60% carbon fibers. They found that at atmospheric pressure, failure was initiated by fiber kinking on the compressive surface of the beams. When the beams were tested under hydrostatic pressure the strength increased with increasing pressure, and at pressures between 150 MPa and 300 MPa (22 and 44 ksi), the failure mode changed to tensile. The strength of the test specimens also increased with increasing pressure for the tensile-dominated failure modes, but not at as high of a rate as the compression-dominated modes (Parry and Wronski 1979, 1981).

Later, Parry and Wronski (1982) studied the behavior of epoxy reinforced with 60% volume fraction carbon fibers in pure compressive tests. Specimens were cut from pultruded rods, then machined into dog bone shapes and tested in the fiber direction. The compressive strength was 1,500 MPa (218 ksi) at atmospheric pressure and increased bilinearly with increasing pressure. For hydrostatic pressures between atmospheric and 150 MPa (22 ksi), the uniaxial fiber direction strength increased at a rate of 0.6 times the applied pressure. For pressures greater than 150 MPa, the fiber direction strength increased at a rate of 3.2 times the applied pressure. The observed failure mode also changed with increasing pressure. Between atmospheric pressure and 150 MPa, fracture appeared to have initiated from longitudinal splitting and was followed by fiber kinking. At higher pressures the main failure mechanism was fiber kinking leading to fiber fracture. The fiber fracture length was between 100 $\mu$m and 400 $\mu$m, much longer than those predicted by Weaver and Williams (1975) for kinking. This led Parry and Wronski to conclude that much of the fiber fracture in Weaver and Williams' work occurred after the failure of the composite due to buckling of the fracture surfaces (Parry and Wronski 1982).

Wronski and Parry (1982) also evaluated the longitudinal compressive strength of epoxy reinforced with 60% volume glass fibers under hydrostatic pressure. Test specimens were prepared in the same manner as in the previous papers (Parry and Wronski 1982). The specimens were loaded in uniaxial

compression at a rate of 0.1 mm/min. The longitudinal compressive strength at atmospheric pressure was 1.15 GPa (162 ksi) and increased at a rate of 3.5 times the applied hydrostatic pressure. At all pressures the failures appeared to be due to kink band formation leading to fiber fracture. Specimens that failed by kink band formation showed a pressure dependence similar to that shown by the carbon-fiber-reinforced specimens that failed through kinking (those that were tested at pressures greater than 150 MPa). This led Wronski and Parry to conclude that kinking shows a much stronger pressure dependence than bundle buckling, so that when kinking became the dominant failure mechanism, the pressure dependence of the longitudinal compressive strength changed at a higher rate (Wronski and Parry 1982).

Sigley, Wronski, and Parry (1992) evaluated the longitudinal compressive strength of pultruded-glass-fiber (52% volume fraction)-reinforced polyester under hydrostatic pressure. Dog bone tensile specimens were manufactured from pultruded rods. These specimens were end loaded at a rate of 0.1 mm/min. Several specimens showed interfacial attack due to the Plexol pressurizing fluid, while the remaining specimens were enclosed in a rubber tubing to prevent the fluid from interacting with the composite.

Three variations of the glass/polyester were evaluated. The first was a Stypol 40-1077 polyester reinforced with 28 × 2400 Equerove glass fiber, and 25% talc as filler. The longitudinal compressive strength at atmospheric pressure for this material was 780 MPa (113 ksi), and the strength increased at a rate of 2.73 times the applied pressure. The second material was a Beetle 811 polyester reinforced with 18 × 2400 tex[*] ECR 1688 glass fiber and 10% calcium carbonate. This material had a longitudinal compressive strength of 380 MPa (55 ksi) at atmospheric pressure and increased at a rate of 2.0 times the applied hydrostatic pressure. The third material was a Beetle 811 polyester reinforced with 9 × 4800 tex ECR 1688 glass fiber and 10% calcium carbonate. The longitudinal compressive strength of this material (450 MPa at atmospheric pressure) increased at a rate of 3.7 times the applied hydrostatic pressure. All of the failure modes exhibited kink band formation followed by fracture along the kink. The fracture surfaces were generally flat and oriented at an angle of 25° to the axis of the fibers (Sigley, Wronski, and Parry 1992).

The yield stresses for the two matrix materials were also evaluated. The yield stress of the Stypol 40-1077 polyester with 25% talc was 120 MPa (17.4 ksi) at atmospheric pressure and increased at a rate of 0.42 times the applied hydrostatic pressure. For the Beetle 811 polyester the yield stress was 80 MPa

---

[*] A fiber designation.

(11.6 ksi) at atmospheric pressure, increased at a rate of 0.16 times the hydrostatic pressure up to 150 MPa (22 ksi), and was constant at higher pressures. The modulus and yield strain increased slightly for the Stypol polyester (0.1% times the hydrostatic pressure and 0.26% times the hydrostatic pressure, respectively), but there was no apparent effect on these properties in the other polymer (Sigley, Wronski, and Parry 1992).

Sigley, Wronski, and Parry (1992) analyzed three failure theories for a composite under hydrostatic pressure, H, with an additional stress, $\sigma_A$, in the fiber direction as shown in Figure 10. First they considered that failure is controlled by the axial compressive strain (as proposed by Steif [1990]). The strain in the fiber direction can be described by equation 11:

$$\varepsilon_1 = \frac{\sigma_1}{E_1} - \frac{2H\upsilon_{tl}}{E_t} ,$$

(11)
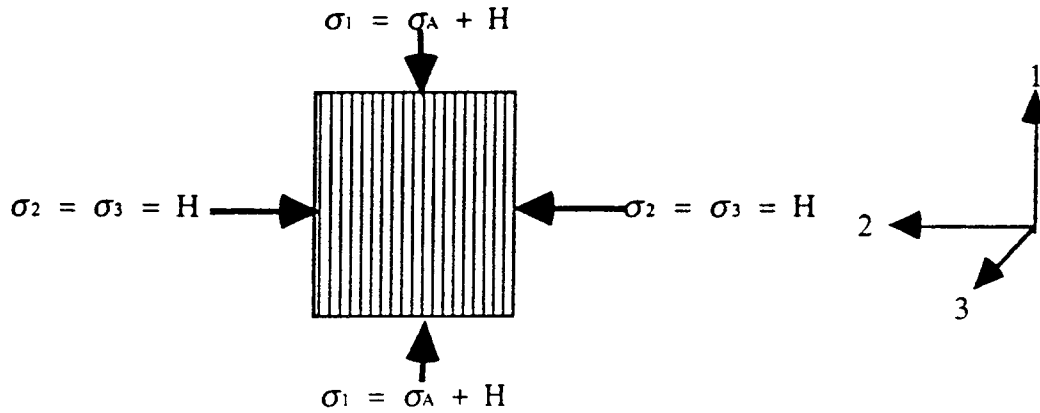


Figure 10. <u>A composite under hydrostatic pressure with an additional stress in the fiber direction.</u>

where $E_1$ is the longitudinal elastic modulus, $E_t$ is the transverse elastic modulus, and $\upsilon_{tl}$ is the Poisson's ratio in the transverse-longitudinal direction. The stress in the fiber direction can then be described by equation 12:

$$\sigma_1 = E_1\varepsilon_1 + 2H\left(\frac{E_1}{E_t}\right)\upsilon_{tl} .$$

(12)

Assuming that $E_1 \cong 5E_t$, and $\upsilon_{tl} = 0.05$, the predicted slope is approximately 0.5, much lower than those observed experimentally (Sigley, Wronski, and Parry 1992).

Sigley, Wronski, and Parry (1992) then analyzed failure controlled by the transverse tensile strains. The strain in the transverse direction can be described by equation 13:

$$\varepsilon_t = \frac{H}{E_t} - \frac{H\upsilon_{tt}}{E_t} - \frac{\sigma_1\upsilon_{lt}}{E_1} . \tag{13}$$

The longitudinal direction stress can then be explicitly defined as:

$$\sigma_1 = H\left(\frac{E_1(1 - \upsilon_{tt})}{\upsilon_{lt}E_t}\right) - \frac{E_1\varepsilon_t}{\upsilon_{lt}} . \tag{14}$$

Assuming $\upsilon_{tt} = 0.3$ and $\upsilon_{lt} = 0.15$, equation 14 gives a pressure dependence of 23.3, much higher than measured (Sigley, Wronski, and Parry 1992).

Finally, Sigley, Wronski, and Parry (1992) derived the pressure dependence due to the transverse deviatoric strain which is given by equation 15:

$$\varepsilon_D = \varepsilon_t - \varepsilon_H , \tag{15}$$

where the hydrostatic strain is described by equation 16:

$$\varepsilon_H = \frac{2H(1 - v_{tt})}{3E_t} - \frac{2Hv_{t1}}{3E_t} - \frac{2\sigma_1v_{lt}}{3E_1} + \frac{\sigma_1}{3E_1} . \tag{16}$$

Substituting equation 16 into 15 yields an expression for the deviatoric strain:

$$\varepsilon_D = \frac{H(1 - v_{tt})}{3E_t} + \frac{2Hv_{t1}}{3E_t} - \frac{\sigma_1v_{lt}}{3E_1} - \frac{\sigma_1}{3E_1} . \tag{17}$$

Solving explicitly for the longitudinal direction stress as a function of the hydrostatic stress,

$$\sigma_1 = \frac{E_1(1 - \nu_{tt} + 2\nu_{tl})}{E_t(1 + \nu_{lt})} H - \frac{3E_1}{(1 + \nu_{lt})} \epsilon_D . \tag{18}$$

If $\nu_{tt} = 0.3$, equation 18 would show that the strength in the longitudinal fiber direction could be increased at a rate of 3.5 times the applied hydrostatic pressure, which was similar to Sigley, Wronski, and Parry's experimental results. It was then proposed that bundle debonding was the critical stage in failure, and once that process had taken place, bundle buckling occurred immediately (Sigley, Wronski, and Parry 1992).

Wronski and Howard (1979) evaluated the tensile and the compressive strength of nickel reinforced with 53% carbon fibers. The longitudinal compressive strength of the material at atmospheric pressure was 930 MPa (135 ksi). Under hydrostatic pressure the strength increased at a rate of 2.9 times the applied pressure up to 100 MPa (14.5 ksi). The failure mode between atmospheric and 100-MPa pressure was by fiber kinking. At higher pressures the failure mode changed to longitudinal splitting of the composite and the strength increased at a rate of 1.0 times the applied pressure (Wronski and Howard 1979).

3.2 Tensile Properties. Parry and Wronski (1985) evaluated the tensile strength of epoxy reinforced with carbon and glass fibers (both were 60% volume fraction) (1986) under hydrostatic pressure. For both materials, the specimens were machined into dog bone shapes from pultruded rods, and tested in tension in the fiber direction under hydrostatic pressure using the test facility described for the compressive tests by Parry and Wronski (1982). For the carbon-fiber-reinforced materials the tensile strength was approximately 2.0 GPa (290 ksi) at atmospheric pressure, and decreased at a rate of 2.0 times the hydrostatic pressure up to 150 MPa, then did not vary with higher pressures. The strain to failure also decreased with increasing pressures. At atmospheric pressure the material showed elastic response up to 1.2 GPa (174 ksi) and nonlinear response, suggesting progressive failure at higher stresses. At 150-MPa applied hydrostatic pressure the material did not show departure from linear behavior until 1.5 GPa (218 ksi) and showed less nonlinear deformation prior to failure. At 300-MPa hydrostatic pressure the material did not show any nonlinear deformation prior to failure (Parry and Wronski 1985).

For the glass-fiber-reinforced materials, the longitudinal tensile strength was 1.7 GPa (247 ksi) at atmospheric pressure and decreased linearly to 1.3 GPa (189 ksi) at 250 MPa (a slope of 1.6 times the hydrostatic pressure). At higher pressures, the strength appeared to be independent of the pressure. The limit of proportionality (limit of elastic behavior) increased linearly with increasing hydrostatic pressure from 0.95 GPa at atmospheric pressures to 1.25 GPa at 300 MPa (a slope of 1.0), so that the material became much more brittle at high pressures. The fracture surface also changed with increasing pressure. At low pressures there was a large amount of fiber pullout as the fibers were fractured at different locations in the specimen gage length. At higher pressures the surface became much flatter and there was less fiber pullout, indicating that failure was more catastrophic (Parry and Wronski 1986).

Experimental observation was made on both materials as explained in terms of the effects of delamination on tensile strength. In tensile tests at atmospheric pressure, when a fiber bundle breaks, the bundle will usually debond from the surrounding matrix. This isolates the crack from the rest of the composite and allows the load to be redistributed into the surrounding fibers. Under high hydrostatic pressure, delamination is suppressed by the large compressive transverse stresses so the crack tip is not blunted from the rest of the material. The stress redistribution between fiber bundles is then suppressed, and the composite fails in a more brittle manner. At high pressures the strengths of both composites do not decrease any more because the matrix becomes completely brittle, and the strength is a function of the minimum fiber bundle strength which is not pressure dependent (Parry and Wronski 1986).

Sigley, Wronski, and Parry (1991) evaluated the tensile properties under hydrostatic pressure of five pultruded-glass-fiber (52% volume fraction)-reinforced composite systems in the fiber direction. For all of the composite systems the tensile fracture strength was initially between 650 and 760 MPa and decreased at a rate between 0.63 and 1.17 times the imposed hydrostatic pressure. The behavior of these five composites under hydrostatic pressure is summarized in Table 4. For each of the materials the limit of proportionality increased, and the amount of fiber pullout decreased with increasing pressure so that failure became more brittle at high pressures. However, unlike the carbon-and-glass fiber-reinforced-epoxy composites mentioned previously, the strength of the polyester matrix composites did not "level off" at high pressures. Sigley, Wronski, and Parry (1991) also reported that this may indicate that the strength of glass fiber bundles may not be independent of hydrostatic pressure, as assumed by Parry and Wronski (1986). Rather, the ultimate strength of the glass fibers may have been controlled by the ultimate strain of the fibers. Under high hydrostatic pressure the transverse stresses cause Poisson's expansion in the principal material direction, increasing the total strain, so that the fibers failed at a lower stress (Sigley, Wronski, and Parry 1991).

24

Parry and Wronski (1990) investigated the effects of hydrostatic pressure on the transverse tensile strength of glass- and carbon-fiber-reinforced epoxy by loading disc-shaped samples in diametral compression. The cylinders were loaded perpendicular to the fiber axis, as shown in Figure 11. Both the glass- and carbon-fiber-reinforced-epoxy samples failed by matrix yielding leading to matrix cracking in the direction to the applied load (in Figure 11, the specimen would fail along a vertical line through the center of the specimen). For glass-fiber-reinforced materials, the transverse strength was 25 MPa (3.6 ksi) at atmospheric pressure and increased at a rate of 0.1 times the hydrostatic pressure. For the carbon-fiber-reinforced composites, the transverse strength was 45 MPa (6.5 ksi) at atmospheric pressure and also increased at a rate of 0.1 times the hydrostatic pressure.


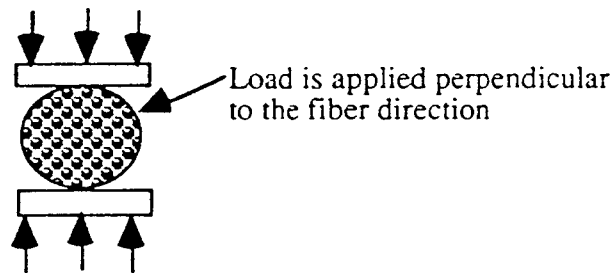
Load is applied perpendicular to the fiber direction

Figure 11. Diametrical compression test.

Yuan et al. (1984) studied the effects of hydrostatic pressure on the tensile behavior of short-glass-fiber-reinforced PVC. The authors tested unreinforced PVC, as well as composites with 10%, 20%, and 30% glass fibers under pressures ranging between atmospheric and 300 MPa (44 ksi). The specimens were injection molded, and the average fiber length was 0.46 mm for the 10% volume fraction and 0.37 mm for the 20% and 30% volume fractions. The specimens were sheathed in Teflon tape and tested in a test chamber which used silicon oil as the pressure transmitting fluid (Yuan et al. 1984).

The moduli of all four experimental materials increased linearly with increasing pressure. The unreinforced PVC had a slope of 3.0; the 10%, 20%, and 30% volume fraction composites had slopes of 3.4, 4.5, and 5.0, respectively. The authors found that the hydrostatic pressure had a minimal effect on the properties of the glass fibers. Thus, the increase in moduli for the composites was due to enhanced adhesion at the interface and improved stress transfer to the fibers. The ductility of the composites increased with increasing hydrostatic pressure, such that the fracture mode changed from brittle to ductile. The ultimate and yield strengths of the unreinforced polymer and the composites also increased with

increasing pressure, although the slopes of the hydrostatic pressure vs. strength curves were not given (Yuan et al. 1984).

Wronski and Howard (1979) evaluated the longitudinal tensile and compressive strengths of nickel reinforced with 53% by volume carbon fibers. The tensile strength of the material at atmospheric pressure was 750 MPa (109 ksi) and did not change when tested under hydrostatic pressure. The tensile failures observed were initiated by fracture of the fibers, followed by fracture of the nickel matrix. Between atmospheric and 140-MPa pressure the nickel matrix failed through necking and transgranular shear. At higher pressures the nickel failed by intergranular parting. The tensile properties of the nickel matrix were also evaluated under hydrostatic pressure. The yield strength of the nickel (270 MPa at atmospheric pressure) did not change with increasing hydrostatic pressure (Wronski and Howard 1979).

Lewandowski et al. (Lewandowski, Liu, and Liu 1991; Liu, Manoharan, and Lewandowski 1989a, 1989b) evaluated the effects of hydrostatic pressure on the tensile behavior of two aluminum alloy systems; one unreinforced, and one reinforced with silicon carbide fibers (15% by volume). The composites and the unreinforced alloys were tested in underaged and overaged conditions at atmospheric pressure and at hydrostatic pressures of 150 and 300 MPa. The tensile strength of the underaged alloy decreased from 683 MPa (100 ksi) at atmospheric pressure to 436 MPa (63 ksi) at an applied hydrostatic pressure of 300 MPa. The strength of the overaged alloy decreased from 572 MPa (83 ksi) at atmospheric pressure to 560 MPa (81 ksi) at 300-MPa applied hydrostatic pressure. Both systems exhibited an increase in ductility and strength when tested under hydrostatic pressure. The strength of the underaged composite increased from 510 MPa (74 ksi) at atmospheric pressure to 719 MPa (104 ksi) at an applied hydrostatic pressure of 300 MPa. The strain to failure of this composite system increased from 10% to 45%. The strength of the overaged composite increased from 482 MPa to 552 MPa (70 to 80 ksi). The strain to failure also increased from 12% to 65%. The fracture surfaces of both composites changed from Mode I at atmospheric pressure to shear failure at 300-MPa hydrostatic pressure (Liu, Manoharan, and Lewandowski 1989b).

3.3 <u>Shear Behavior.</u>

3.3.1 In-Plane Shear. Parry and Wronski (1982) studied the interlaminar shear strength of epoxy reinforced with 60% volume fraction carbon fibers and later the interlaminar shear strength of epoxy reinforced with 60% glass fibers (Wronski and Parry 1982). In-plane shear tests were conducted on

double-notch shear specimens with notches cut perpendicular to the fiber direction. The specimens were loaded in the fiber direction as shown in Figure 12. For the carbon-fiber-reinforced specimens the shear strength was 75 MPa at atmospheric pressure and increased at a rate of 0.25 times the hydrostatic pressure up to 150 MPa. At higher pressures the shear strength increased at a higher rate; however, the mode of failure changed to kinking of the fibers so that the failure was no longer shear, so instead the test could be described as a notched compressive test (Parry and Wronski 1982).
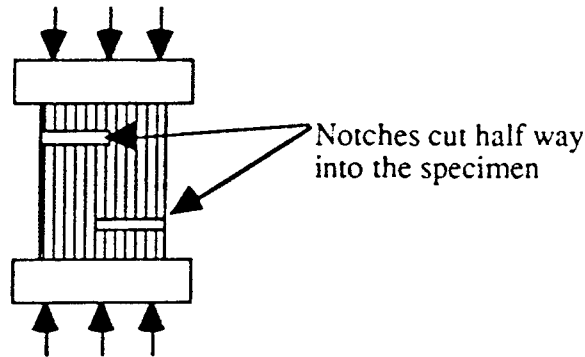


Figure 12. In-plane shear test.

For the glass-fiber-reinforced specimens, the in-plane shear strength was 42 MPa at atmospheric pressure and increased at a rate of 0.2 times the applied hydrostatic pressure. The failure mode was shear at all pressures. The authors indicated that in the carbon-fiber-reinforced epoxy under high hydrostatic pressure, the stresses were high enough to initiate matrix yielding, then kinking of the fibers, thus causing the failure to be compressive. In the glass-fiber-reinforced composites, the stresses were much lower and shear failure occurred prior to matrix yielding (Parry and Wronski 1982) .

3.3.2 Torsional Shear. Shin and Pae (1992b), and later, Weng and Pae (1992) studied the mechanical response of graphite-fiber (60% volume fraction)-reinforced epoxy and unreinforced epoxy specimens tested in torsion at hydrostatic pressures up to 700 MPa (102 ksi). Several specimen configurations were examined, including the following: unreinforced epoxy specimens, 0° laminated specimens (Shin and Pae 1992b), and +45°, −45°, and 90° filament-wound specimens (Shin and Pae 1992a). The composites were manufactured from Scotchply SP-319 preimpregnated tape, which contained Thornel 300 graphite fibers and PR-319 epoxy. The 0° test specimens were prepared from 0.5-in-thick laminates cut as rectangular specimens, then the gage sections were machined into an hourglass shape. The centers of the specimens were drilled out to prevent a site of high stress concentration during the torsional testing. A diagram of

27

the test specimen is shown in Figure 13. The other composite test specimens were filament wound onto a copper mandrel, which was removed prior to testing. All specimens were dipped in a rubber latex/toluene solution to prevent interaction with the pressurizing fluid (Dow Corning 200 silicon oil). The testing apparatus (described in detail in Shin and Pae [1992b]) provided for constant hydrostatic pressure during all testing and allowed the test specimens to move freely so that torsional loads could be applied independent of axial loads.
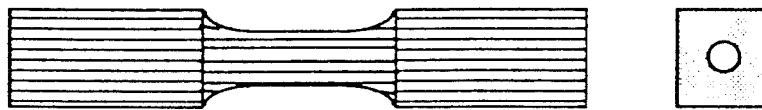
from Shin & Pae, J. of Composite
Materials, V.26, n.4, p.475 (1992)

Figure 13. Composite torsional test specimen.

In all of the composites and unreinforced epoxy the shear strength, shear modulus, and shear strain to failure increased with increasing hydrostatic pressure. The properties generally showed a bilinear curve with respect to hydrostatic pressure increasing at a high linear rate up to 200 MPa (29 ksi), then increasing at a lower linear rate at pressures above 200 MPa. The transition point at 200 MPa was attributed to the hydrostatic-pressure-induced shifting of the glass transition of the epoxy (Pae and Bhateja 1975; Shin and Pae 1992b; Shin and Pae 1992a; Sauer 1977).

The unreinforced epoxy behaved in a brittle manner at hydrostatic pressures less than 100 MPa (14.5 ksi), where all specimens failed catastrophically. At higher pressures the epoxy showed some nonlinear response at higher stresses, and the final failure was usually due to a single crack at 45° to the longitudinal axis (along the plane of maximum tensile stress). These changes in the failure behavior indicated that the higher pressure suppressed the initiation and growth of cracks in the material, allowing the material to deform through shear yielding prior to failure. The strength of the epoxy increased at a rate of 0.1 times the hydrostatic pressure up to 200 MPa. At higher pressures the strength of the epoxy increased at 0.033 times the pressure.

The unidirectional (0°) systems also showed increasing nonlinear deformation and strength with increasing pressure. Shear stress vs. shear strain curves for the composites tested under several levels of hydrostatic pressure are shown in Figure 14. The strength of the specimens were 71 MPa at atmospheric
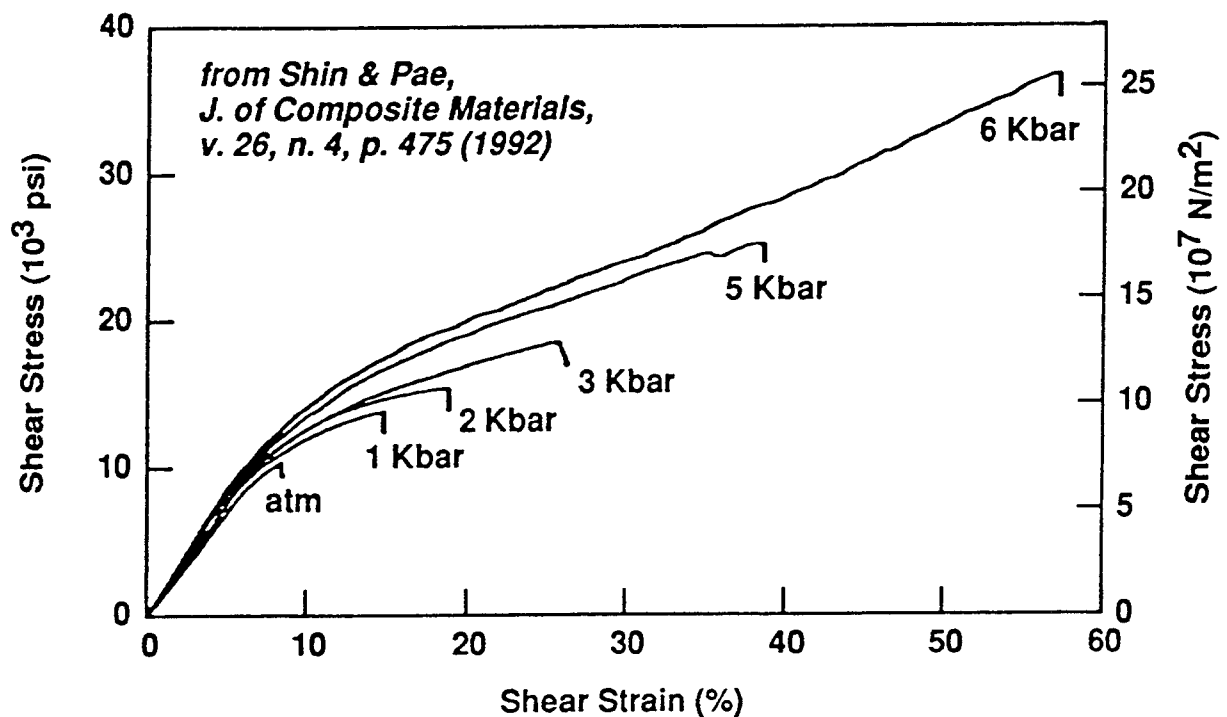
28

Figure 14. Shear stress vs. shear strain curves for torsional test on unidirectional-graphite-fiber-reinforced epoxy.

pressure and increased at a rate of 0.17 times the applied hydrostatic pressure. At pressures greater than 400 MPa, the specimens deformed through over 50° of rotation. This caused a change in failure mode from fiber-matrix-dominated failure to fiber fracture. The specimens that failed in a fiber-dominated mode had an average strength of 228 MPa, which did not appear to vary with hydrostatic pressure. The shear modulus of the 0° specimens increased from 1.07 GPa at atmospheric pressure at a rate of 0.26 times the applied hydrostatic pressure up to 200 MPa and 0.21 times the applied pressure at higher pressures (Shin and Pae 1992b).

When 90° specimens are loaded in torsional shear the local stresses should be the same as those on the 0° specimens. However, as noted above, the 0° and 90° specimens were manufactured through different techniques, and this may account for significant differences in the observed mechanical properties. The average strength of the 90° samples was 100 MPa (14.5 ksi) at atmospheric pressure and increased at a rate of 0.121 times the applied pressure at pressures up to 200 MPa. At higher pressures the strength increased at a rate of 0.046 times the applied pressure. The shear modulus increased at a rate of 0.24 up to 200-MPa applied hydrostatic pressure, and 0.22 from 200- to 600-MPa applied hydrostatic pressure, which was very close to the values found for the torsion tests on 0° specimens (Shin and Pae 1992a).

When the +45° specimens were loaded in torsion there were tensile stresses in the fiber direction and compressive stresses transverse to the fibers. At low pressures the specimens failed by matrix-dominated cracking, and the strength was 167.5 MPa (24 ksi) at atmospheric pressure and increased at a rate of 0.16 times the applied pressure. Specimens tested at higher pressures failed by a combination of fiber and matrix fracture, and the reported fracture strengths were much higher (approximately 250 MPa) (Shin and Pae 1992a).

In the −45° specimens loaded in torsion, the principal tensile stress is transverse to the fiber direction and the mechanical properties are much lower than those of the +45° specimens. All of the −45° specimens failed through matrix cracking. The shear strength was 21 MPa at atmospheric pressure and increased at a rate of 0.09 times the applied pressure up to an applied hydrostatic pressure of 200 MPa, and 0.04 times the applied pressure at higher pressures (Shin and Pae 1992a).

## 4. DISCUSSION

High hydrostatic pressure can affect a composite in several ways. First, it can affect the individual constituents. Most of the polymers discussed in section 2 of this report show a strong pressure dependence with the strength, stiffness, and yield strength increasing with increasing hydrostatic pressure. Most studies have indicated that pressure has no or very little effect on the glass or graphite fibers themselves. The only exception to this is the article by Sigley, Wronski, and Parry (1991), which reported that the glass fibers were weak in tension under hydrostatic pressure due to the high transverse stresses. A second effect of the pressure is that it increases the interfacial normal and shear stresses, thus increasing the adhesion between the fibers and the matrix. Finally, the hydrostatic pressure can reduce the influence of flaws such as microcracks, voids, and delaminations in composites by effectively closing the flaws and increasing the amount of work needed for crack growth (Shin and Pae 1992a).

4.1 Compression Behavior. The compressive behavior of composites, as described in section 3.1, shows a stronger dependence on the hydrostatic pressure than either the tensile or shear properties. Table 3 contains a summary of the atmospheric compressive strengths of these materials and the slopes of the strength vs. applied pressure curves. Figure 15 shows these results graphically. It is noted that all of the polymer matrix composites evaluated were unidirectional and made through pultrusion. This process can cause poor fiber placement (large amounts of fibers in bundles or poorly aligned fibers) in the final specimen. The properties of these composites under hydrostatic pressure may not be the same

30

Table 3. The Effects of Hydrostatic Pressure on the Compressive Strengths of Composites

| Matrix | Fiber ($V_f$) | Reference | Atm. Strength (MPa) | Slope 1 (mode) | Inflection (MPa) | Slope 2 (mode) |
|---|---|---|---|---|---|---|
| epoxy | carbon (36%) | Weaver and Williams 1975 | 511 | 3.2 (splitting) | 100 | 1.0 (kinking) |
| epoxy | carbon (60%) | Parry and Wronski 1982 | 1,500 | 0.6 (splitting | 150 | 3.2 (kinking) |
| epoxy | glass (60%) | Parry and Wronski 1982 | 1,150 | 3.5 (kinking) | — | — |
| Stypol 40-1077 polyester (yield strength) | — | Sigley, Wronski, and Parry 1992 | 120 | 0.42 | — | — |
| Stypol 40-1077 polyester | 28 × 2,400 Equerove glass (52%) | Sigley, Wronski, and Parry 1992 | 780 | 2.73 (kinking) | — | — |
| Beetle 811 polyester (yield strength) | — | Sigley, Wronski, and Parry 1992 | 80 | 0.16 | — | — |
| Beetle 811 polyester | 19 × 2,400 tex ECR 1688 glass (52%) | Sigley, Wronski, and Parry 1992 | 380 | 2.0 (kinking) | — | — |
| Beetle 811 polyester | 9 × 4,800 tex ECR 1688 glass (52%) | Sigley, Wronski, and Parry 1992 | 450 | 3.7 (kinking) | — | — |
| nickel | Type II carbon (53%) | Wronski and Howard 1979 | 930 | 2.9 (kinking) | 100 | 1.10 (splitting) |

as those for composites with better fiber alignment. In addition to this, all of the specimens tested were dog bone shaped, and loaded from the end. While these studies did not address the importance of specimen geometry on the test results, other studies (Camponeschi 1991) have indicated that compressive strength of composite materials is strongly dependent on specimen geometry.

Several of the composites listed in Table 3 show a change in slope of the hydrostatic pressure vs. unidirectional compression strength curves. While this type of change in slope is attributed to a glass or secondary transition in the unreinforced polymer, in the composites this is attributed to a change in the failure mechanism. In an analysis of the compressive failure of composite, Piggott (1981) described six possible failure mechanisms. While each mechanism will be affected in a different manner, the mechanism with the lowest strength will dominate failure of the composite.
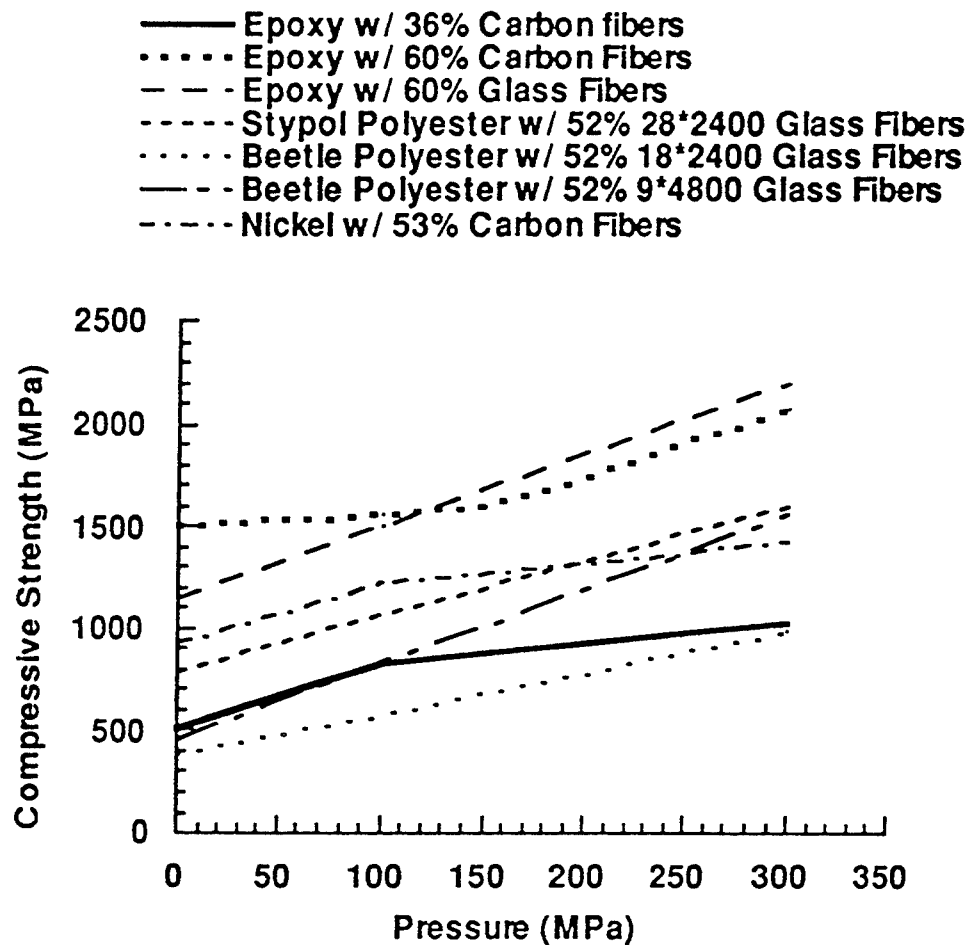
Figure 15. Compressive strength vs. hydrostatic pressure for several continuous-fiber-reinforced composites.

The two dominate failure mechanisms in the experimental work are splitting of the composite and fiber kinking leading to ultimate failure. In the work by Weaver and Williams (1975), the uniaxial compressive strengths of the composites that fail through kinking increase at a rate of 1.0 times the applied hydrostatic pressure, and the strengths of those that fail by splitting increase at a rate of 2.9 times the applied hydrostatic pressure. In the work by Wronski et al. (Sigley, Wronski, and Parry 1992; Parry and Wronski 1982; Wronski and Parry 1982; Wronski and Howard 1979), the strengths of composites that fail through kinking increase at rates between 2.0 and 3.5 times the hydrostatic pressure, and the strengths of those that fail by splitting increase at rates between 0.6 and 1.0. The changes in pressure dependence in these mechanisms may also be influenced by the different fiber volume fractions. Weaver and Williams (1975) worked with composite systems with 36% fiber volume fraction, and Wronski et al. (Sigley, Wronski, and Parry 1992; Parry and Wronski 1982; Wronski and Parry 1982; Wronski and Howard 1979) worked with systems with between 52% and 60% fiber volume fraction.

The increased strength of the composites could be due to several mechanisms. The increased stiffness and yield strength of the matrix would increase the stress necessary to initiate bundle buckling and kinking in the composite. Portelli et al. (1992) have shown that the compression strength of composites is strongly dependent on the modulus of the matrix. They found that by increasing the test temperature they reduced the shear modulus of the matrix and subsequently reduced the compressive strength of the composite material. Another important effect of the hydrostatic pressure is the high transverse stresses which increase the interfacial adhesion, making the composite more resistant to splitting failure.

4.2 <u>Tensile Behavior</u>. The unidirectional tensile strengths of the composites reviewed, along with the slopes of the strength vs. hydrostatic pressure curves, are given in Table 4. These results are shown in Figure 16. Unlike the strengths of the unreinforced polymers and the compressive strengths of the composites, the tensile strengths of the composites do not always increase with increasing pressure. Parry and Wronski (1985, 1986) reported that the decrease in strength for the continuous-fiber-reinforced composites was due to the increased yield strength and corresponding decrease in toughness of the matrix material. Under high pressure the matrix becomes brittle and is not able to blunt cracks, so when one fiber bundle fails the entire composite fails catastrophically. The work by Wronski and Pick (1977) on carbon-fiber-reinforced nickel reinforces this theory: the yield stress of the nickel matrix did not change under hydrostatic pressure, and the strength of the composite was also unaffected by pressure. It is important to note that while the tensile strength of the composites decreased with increasing pressure, the point of nonlinear response (due to first bundle failure) increased. Therefore, if the point of nonlinear response is considered to be the point of failure for a composite, then the failure criterion increases with increasing pressure. Since the strength of composites is often controlled by the minimum bundle strength, tension tests on composites with better fiber alignment and distribution may show a different pressure dependence than pultruded composite systems.

In the short-fiber-reinforced PVC evaluated by Yuan et al. (1984) and the particle-reinforced alloys studied by Liu, Manoharan, and Lewandowski (1989b), the tensile strengths increased with increasing hydrostatic pressure. This is significant because the unreinforced PVC does not show as high of a pressure dependence as the fiber-reinforced PVC, and the strengths of the aluminum alloys actually decrease with increasing hydrostatic pressure. The strength of these systems must then increase due to the enhanced adhesion at the interfaces and the suppression of crack growth in the materials.

Table 4. The Effects of Hydrostatic Pressure on the Tensile Strengths of Composites

| Matrix | Fiber (V$_f$) | Reference | Atm. Strength (MPa) | Slope 1 | Inflection (MPa) | Slope 2 |
|---|---|---|---|---|---|---|
| epoxy | carbon (60%) | Parry and Wronski 1985 | 2,000 | −2.0 | 150 | 0.0 |
| epoxy | glass (60%) | Parry and Wronski 1986 | 1,700 | −1.6 | 250 | 0.0 |
| Stypol 40-1077 polyester | 28 × 2,400 Equerove glass (52%) | Sigely, Wronski, and Parry 1991 | 700 | −0.75 | — | — |
| Stypol 40-1077 polyester | 28 × 2,400 Equerove 23/47 glass (52%) | Sigley, Wronski, and Parry 1991 | 650 | −0.63 | — | — |
| Stypol 40-1077 polyester | 28 × 2,400 R099 glass (52%) | Sigley, Wronski, and Parry 1991 | 660 | −0.65 | — | — |
| Beetle 811 polyester | 18 × 2,400 tex ECR 1688 glass (52%) | Sigley, Wronski, and Parry 1991 | 730 | −1.17 | — | — |
| Beetle 811 polyester | 9 × 4,800 tex ECR 1688 glass (52%) | Sigley, Wronski, and Parry 1991 | 760 | −1.06 | — | — |
| nickel | carbon (53%) | Wronski and Howard 1979 | 750 | — | — | — |

4.3 Shear Behavior. The shear strength of the composite materials, summarized in Table 5, does not show as strong of a hydrostatic pressure dependence as either the tensile or compressive strength. These moderate increases could be due to the increased shear modulus of the matrix materials, enhanced adhesion at the fiber/matrix interface in the composites, and by the suppression of crack growth in the composite materials.

5. CONCLUSIONS

Hydrostatic pressure can significantly influence the mechanical behavior of unreinforced and reinforced polymers. The strength, stiffness, and yield strength of polymers generally increase with increasing applied hydrostatic pressure. In composite materials the effects of hydrostatic pressure depended on the type of test and the constituents of the material. In the compression tests the unidirectional strengths of the composites always increased when tested under pressure. The rate at which the strength increased depended on the failure mode of the composites. Wronski et al. (Sigley, Wronski, and Parry 1992; Parry
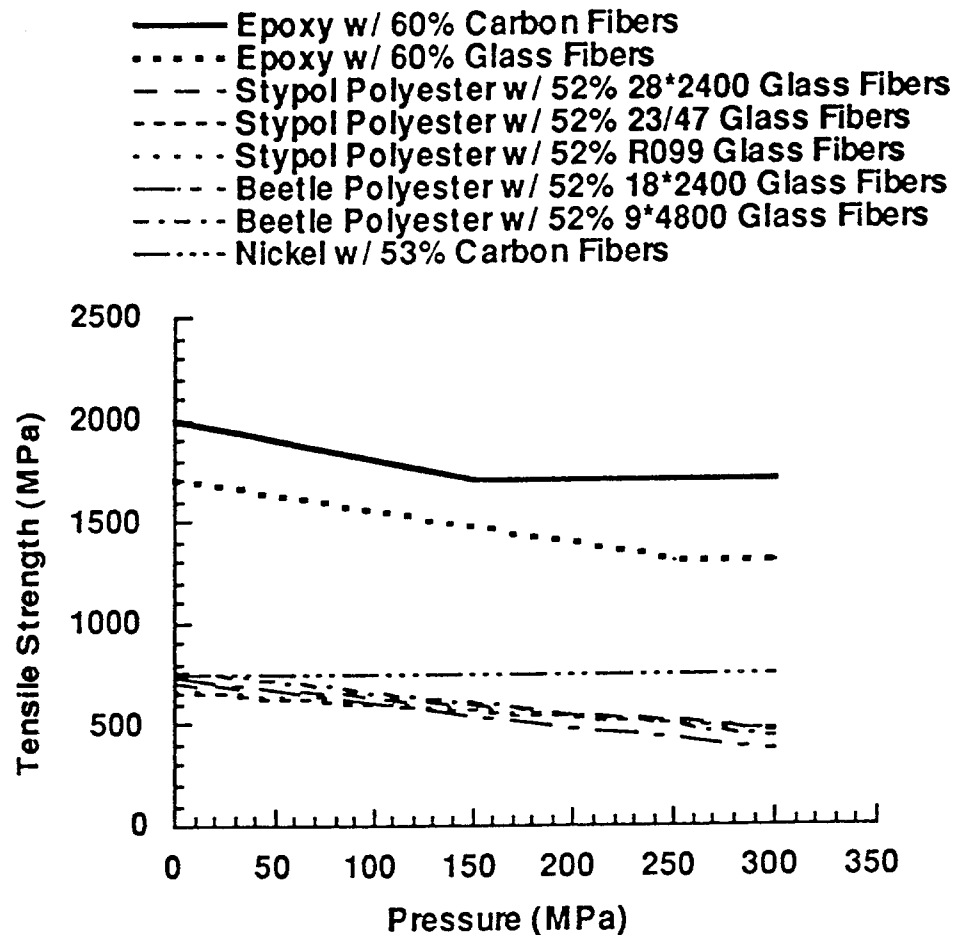
Figure 16. Tensile strength vs. hydrostatic pressure for several continuous-fiber-reinforced composites.

and Wronski 1982; Wronski and Parry 1982; Wronski and Howard 1979) found that the strength of composites that failed through kinking increased at a rate of approximately three times the applied pressure while those that failed through splitting increased at a rate of approximately one times the hydrostatic pressure. Weaver and Williams (1975) found that the strength of composites that failed through kinking increased at a rate of approximately one times the applied hydrostatic pressure and that those with splitting failure had strengths which increased at a rate of approximately three times the applied hydrostatic pressure.

The tensile strengths of continuous-fiber-reinforced polymers generally decreased with increasing pressure due to reduced toughness of the matrices. However, the tensile strengths of discontinuous-fiber-reinforced composites generally increased due to the enhanced interfacial adhesion and reduced crack growth caused by the hydrostatic pressure. The shear behavior of the composites that were evaluated was less sensitive to the effects of hydrostatic pressure than the tensile or compressive behaviors. However, the shear stiffness and strengths did exhibit slight increases with increasing hydrostatic pressure.

Table 5. The Effects of Hydrostatic Pressure on the Shear Strengths of Composites

| Matrix | Fiber (Vf) | Type of Test | Reference | Atm. Strength (MPa) | Slope 1 | Inflection (MPa) | Slope 2 |
|---|---|---|---|---|---|---|---|
| epoxy | carbon (60%) | In-plane shear | Parry and Wronski 1982 | 75 | 0.25 | 150 | — |
| epoxy | glass (60%) | In-plane shear | Wronski and Parry 1982 | 42 | 0.2 | — | — |
| epoxy | — | Torsion | Shin and Pae 1992b | 37.9 | 0.100 | 200 | 0.033 |
| epoxy-matrix mode | graphite (60%) | 0° Torsion | Shin and Pae 1992b | 71.0 | 0.170 | — | — |
| epoxy-fiber mode | graphite (60%) | 0° Torsion | Shin and Pae 1992b | 228 | — | — | — |
| epoxy | graphite (60%) | 90° Torsion | Shin and Pae 1992a | 100 | 0.121 | 200 | 0.046 |
| epoxy-matrix mode | graphite (60%) | +45° Torsion | Shin and Pae 1992a | 167.5 | 0.16 | — | — |
| epoxy-fiber mode | graphite (60%) | +45° Torsion | Shin and Pae 1992a | 246.3 | 0.06 | — | — |
| epoxy | graphite (60%) | −45° Torsion | Shin and Pae 1992a | 21.1 | 0.09 | 200 | 0.04 |

# 6. REFERENCES

Agarwal, B. D., and L. J. Broutman. Analysis and Performance of Fiber Composites. New York: John Wiley & Sons, 1980.

Bhateja, S. K., and K. D. Pae. "Effects of Hydrostatic Pressure on the Mechanical Behavior of Polyimide." Journal of Polymer Science, Polymer Letters, vol. 10, pp. 551–555, 1972.

Biglione, G., E. Baer, and S. V. Radcliffe. "Effects of High Hydrostatic Pressure on the Mechanical Behavior of Homogeneous and Rubber Reinforced Amorphous Polymers." Proceedings of the Second International Conference on Fracture, 1969.

Birch, F. "The Effect of Pressure Upon the Elastic Parameters of Isotropic Solids, According to Murnaghan's Theory of Finite Strain." Journal of Applied Physics, vol. 9, no. 4, pp. 279–288, 1938.

Bridgman, P. W. The Physics of High Pressure, 3rd ed. London: Bell, 1958.

Brown, E. T. (editor) "Suggested Methods for Determining the Strength of Rock Materials in Triaxial Compression in Rock Characterization Testing and Monitoring." Elmsford, NJ: Pergamon Press Inc., pp. 125–127, 1981.

Caddell, R. M., R. S. Raghava, and A. G. Atkins. "Pressure Dependent Yield Criteria for Polymers." Materials Science and Engineering, vol. 13, pp. 113–120, 1974.

Camponeschi, E. T., Jr. "Compression of Composite Materials: A Review in Composite Materials: Fatigue and Fracture." ASTM STP 1110, American Society for Testing Materials, Philadelphia, PA, 1991.

Christiansen, A. W., E. Baer, and S. V. Radcliffe. "The Mechanical Behavior of Polymers Under High Pressure." Philisophical Magazine, vol. 24, pp. 451–467, 1971.

Gol'dman, A. Ya., G. E. Mesh, and A. G. Korchagin. "Effect of Hydrostatic Pressure on the Damage Accumulation Process in Polyethylene Extended Under Pressure." Mechanics of Composite Materials, vol. 21, no. 5, pp. 517–521, 1985.

Heard, H. C. "Effect of Large Changes in Strain Rate in the Experimental Deformation of Yule Marble." Journal of Geology, vol. 71, pp. 162–195, 1963.

Hu, L. W., and K. D. Pae. "Inclusion of the Hydrostatic Stress Component in Formulation of the Yield Condition." Journal of the Franklin Institute, vol. 275, pp. 491–502, 1963.

Laka, M. G., and A. A. Dzenis. "Effect of Hydrostatic Pressure on the Tensile Strength of Polymer Materials." Polymer Mechanics, vol. 3, no. 6, pp. 685–687, 1967.

Lewandowski, J. J., D. S. Liu, and C. Liu. "Observations on the Effects of Particulate Size and Superposed Pressure on Deformation of Metal Matrix Composites." Scripta Metallurgica, vol. 25, pp. 21-26, 1991.

Liu, D. S., M. Manoharan, and J. J. Lewandowski. "Effects of Microstructure on the Behavior of an Aluminum Alloy and an Aluminum Matrix Composite Tested Under Low Levels of Superimposed Hydrostatic Pressure." Metallurgical Transactions A, vol. 20A, pp. 2409–2417, 1989a.

Liu, D. S., M. Manoharan, and J. J. Lewandowski. "Effects of Superimposed Hydrostatic Pressure on the Fracture Properties of Particulate Reinforced Metal Matrix Composites." Scripta Metallurgica, vol. 23, pp. 253–256, 1989b.

Matsushige, K., S. V. Radcliffe, and E. Baer. Journal of Materials Science, vol. 10, p. 833, 1975.

Mears, D. R., K. D. Pae, and J. A. Sauer. "Effects of Hydrostatic Pressure on the Mechanical Behavior of Polyethylene and Polypropylene." Journal of Applied Physics, vol. 40, no. 11, pp. 4229–4237, 1969.

Murnaghan, F. D. "Finite Deformations of an Elastic Solid." American Journal of Mathematics, vol. 59, pp. 235–260, 1937.

Murnaghan, F. D. Finite Deformation of an Elastic Solid. Applied Mathematics Series. Edited by I. S. Sokolnikoff. New York: John Wiley & Sons, Inc., 1951.

Pae, K. D. "The Macroscopic Yielding Behavior of Polymers in Multiaxial Stress Fields." Journal of Materials Science, vol. 12, pp. 1209–1214, 1977.

Pae, K. D., and S. K. Bhateja. "The Effects of Hydrostatic Pressure on the Mechanical Behavior of Polymers." Journal of Macromolecular Science, Part C, Reviews in Macromolecular Chemistry, vol. C13, pp. 1–75, 1975.

Pae, K. D., and J. A. Sauer. "Influence of Pressure on the Elastic Modulus, the Yield Strength, and the Deformation of Polymers." Engineering Solids Under Pressure. Presented at the Third International Conference on High Pressure, Institution of Mechanical Engineering, Aviemore, Scotland, 1970.

Parry, T. V., and A. S. Wronski. "The Effect of Hydrostatic Pressure on Transverse Strength of Glass and Carbon Fibre-Epoxy Composites." Journal of Materials Science, vol. 25, pp. 3162–3166, 1990.

Parry, T. V., and A. S. Wronski. "The Tensile Properties of Pultruded GRP Tested Under Superposed Hydrostatic Pressure." Journal of Materials Science, vol. 21, pp. 4451–4455, 1986.

Parry, T. V., and A. S. Wronski. "Failure of Carbon Fibre Reinforced Plastic Under Superposed Pressure in Three-Point Bending." High Pressure Science and Technology, Proceedings of the VIIth International AIRAPT Conference, Le Creusot, France, 1979.

Parry, T. V., and A. S. Wronski. "Kinking and Compressive Failure in Uniaxially Aligned Carbon Fibre Composite Tested Under Superposed Hydrostatic Pressure." Journal of Materials Science, vol. 17, pp. 893–900, 1982.

Parry, T. V., and A. S. Wronski. "The Effect of Hydrostatic Pressure on the Tensile Properties of Pultruded CFRP." Journal of Materials Science, vol. 20, pp. 2141–2147, 1985.

Parry, T. V., and A. S. Wronski. "Kinking and Tensile, Compressive and Interlaminar Shear Failure in Carbon-Fibre-Reinforced Plastic Beams Tested in Flexure." Journal of Materials Science, vol. 16, pp. 439-450, 1981.

Paterson, M. S. "Effect of Pressure on Young's Modulus and the Glass Transition in Rubbers." Journal of Applied Physics, vol. 35, no.1, pp. 176–179, 1964.

Piggott, M. R. "A Theoretical Framework for the Compressive Properties of Aligned Fibre Composites." Journal of Materials Science, vol. 16, pp. 2837–2845, 1981.

Portelli, G. B., D. P. Goetz, J. A. Graske, and A. M. Hine. "The Effect of Matrix Modulus on Lamina Compression Strength." Paper presented at the 37th International SAMPE Symposium and Exhibition, Society for the Advancement of Material and Process Engineering, Anaheim, CA, 1992.

Sauer, J. A. "Deformation, Yield, and Fracture of Polymers at High Pressure." Polymer Engineering and Science, vol. 17, no. 3, pp. 150–164, 1977.

Sauer, J. A., K. D. Pae, and S. K. Bhateja. "Influence of Pressure on the Yield and Fracture of Polymers." Journal of Macromolecular Science - Physics, vol. B8, no. 3-4, pp. 631–654, 1973.

Shin, E. S., and K. D. Pae. "Effects of Hydrostatic Pressure on In-Plane Shear Properties of Graphite/ Epoxy Composites." Journal of Composite Materials, vol. 26, no. 6, pp. 828–868, 1992a.

Shin, E. S., and K. D. Pae. "Effects of Hydrostatic Pressure on the Torsional Shear Behavior of Graphite/ Epoxy Composites." Journal of Composite Materials, vol. 26, no. 4, pp. 462–485, 1992b.

Sigley, R. H., A. S. Wronski, and T. V. Parry. "Axial Compressive Failure of Glass-Fibre Polyester Composites Under Superposed Hydrostatic Pressure: Influence of Fibre Bundle Size." Composite Science and Technology, vol. 43, pp. 171-183, 1992.

Sigley, R. H., A. S. Wronski, and T. V. Parry. "Tensile Failure of Pultruded Glass-Polyester Composites Under Superimposed Hydrostatic Pressure." Composites Science and Technology, vol. 41, pp. 395–409, 1991.

Silano, A. A., S. K. Bhateja, and K. D. Pae. "Effects of Hydrostatic Pressure on the Mechanical Behavior of Polymers: Polyurethane, Polyoxymethylene, and Branched Polyethylene." International Journal of Polymeric Materials, vol. 3, pp. 117–131, 1974.

Silano, A. A., and K. D. Pae. "The Influence of Pressure on the Mechanical Behavior of Polychlorotrifluoroethylene." Advances in Polymer Science and Engineering. New York: Plenum Press 1972.

Steif, P. S. "A Model for Kinking in Fiber Composites-II. Kink Band Formation." International Journal of Solids and Structures, vol. 26, no. 5/6, pp. 563–569, 1990.

Sternstein, S. S., and L. Ongchin. Polymer Reprints of the American Chemical Society, Division of Polymer Chemistry, vol. 10, p. 117, 1969.

Sweeney, J., R. A. Duckett, and I. M. Ward. "The Fracture Behavior of uPVC at both Ambient and High Hydrostatic Pressures." Journal of Materials Science, vol. 20, pp. 3705–3715, 1985.

Sweeney, J., R. A. Duckett, and I. M. Ward. "Fracture Toughness of a Tough Polyethylene Using Tension Testing in a High-Pressure Environment." Journal of Materials Science Letters, vol. 5, no. 11, pp. 1109–1110, 1986.

Sweeney, J., R. A. Duckett, and I. M. Ward. "The Fracture Behavior of Oriented Polyethylene at High Pressures." Proceedings of the Royal Society of London, series A, vol. 420, pp. 53–80, 1988.

Sweeney, J., R. A. Duckett, I. M. Ward, and J. G. Williams. "Plastic Zone Corrections in Relation to Fracture Measurements in Torsion on Tough Polyethylenes." Journal of Materials Science Letters, vol. 4, pp. 217–220, 1985.

Truss, R. W., R. A. Duckett, and I. M. Ward. "The Fracture Toughness of Tough Polyethylenes by a Novel High Pressure Technique." Journal of Materials Science, vol. 19, pp. 413–422, 1984.

Vodar, B., and J. Kieffer. Historical Introduction, the Mechanical Behavior of Materials Under Pressure." Edited by H.Ll.D. Pugh. London: Applied Science Publishers, Ltd., pp. 1–53, 1971.

Weaver, C. W., and J. G. Williams. "Deformation of a Carbon-Epoxy Composite Under Hydrostatic Pressure." Journal of Materials Science, vol. 10, pp. 1323–1333, 1975.

Weng, G. J., and K. D. Pae. "Pressure-Induced Nonlinear Behavior of Fiber-Reinforced Composites." Mechanics of Composites Review, 1992.

Wronski, A. S., and M. Pick. "Pyramidal Yield Criteria for Epoxies." Journal of Materials Science, vol. 12, pp. 28–34, 1977.

Wronski, A. S., and T. V. Parry. "Compressive Failure and Kinking in Uniaxially Aligned Glass-Resin Composite Under Superposed Hydrostatic Pressure." Journal of Materials Science, vol. 17, pp. 3656–3662, 1982.

Wronski, A. S., and R. J. Howard. "Tensile and Compressive Strengths of Uniaxially-Aligned Carbon Fibre-Nickel Composite Under Superposed Hydrostatic Pressure." Proceedings of the VIIth International AIRAPT Conference, Le Creusot, France, 1979.

Yoon, H. N., K. D. Pae, and J. A. Sauer. "Hydrostatic Extrusion of Polypropylene and Properties of Extrudates." Polymer Engineering and Science, vol. 16, p. 567, 1976.

Yuan, J., A. Hiltner, E. Baer, and D. Rahrig. "The Effect of High Pressure on the Mechanical Behavior of Short Fiber Composites." Polymer Engineering and Science, vol. 24, no. 11, pp. 844–850, 1984.

# LIST OF ABBREVIATIONS

| | |
|---|---|
| ABS | Acrylonitrile butadiene styrene |
| CA | Cellulose acetate |
| HIPS | High-impact polystyrene |
| LDPE | Low-density polyethylene |
| MDPE | Medium-density polyethylene |
| PE | Polyethylene |
| PC | Polycarbonate |
| PCTFE | Polychlorotrifluoroethylene |
| PI | Polyimide |
| PMMA | Polymethyl methacrylate |
| POM | Polyoxymethylene |
| PP | Polypropylene |
| PTFE | Polytetrafluoroethylene |
| PU | Polyurethane |
| PVC | Polyvinyl chloride |

INTENTIONALLY LEFT BLANK.

NO. OF
COPIES   ORGANIZATION

2      ADMINISTRATOR
       ATTN DTIC DDA
       DEFENSE TECHNICAL INFO CTR
       CAMERON STATION
       ALEXANDRIA VA 22304-6145

1      DIRECTOR
       ATTN AMSRL OP SD TA
       US ARMY RESEARCH LAB
       2800 POWDER MILL RD
       ADELPHI MD 20783-1145

3      DIRECTOR
       ATTN AMSRL OP SD TL
       US ARMY RESEARCH LAB
       2800 POWDER MILL RD
       ADELPHI MD 20783-1145

1      DIRECTOR
       ATTN AMSRL OP SD TP
       US ARMY RESEARCH LAB
       2800 POWDER MILL RD
       ADELPHI MD 20783-1145


       ABERDEEN PROVING GROUND

5      DIR USARL
       ATTN AMSRL OP AP L (305)

| NO. OF COPIES | ORGANIZATION |
|---|---|
| 1 | HQDA<br>ATTN SARD TT DR F MILTON<br>PENTAGON<br>WASHINGTON DC 20310-0103 |
| 1 | HQDA<br>ATTN SARD TT MR J APPEL<br>PENTAGON<br>WASHINGTON DC 20310-0103 |
| 1 | HQDA<br>ATTN SARD TT MS C NASH<br>PENTAGON<br>WASHINGTON DC 20310-0103 |
| 1 | HQDA<br>ATTN SARD TR DR R CHAIT<br>PENTAGON<br>WASHINGTON DC 20310-0103 |
| 1 | HQDA<br>ATTN SARD TR MS K KOMINOS<br>PENTAGON<br>WASHINGTON DC 201310-0103 |
| 1 | DIRECTOR<br>ATTN AMSRL CP CA D SNIDER<br>US ARMY RESEARCH LAB<br>2800 POWDER MILL ROAD<br>ADELPHI MD 20783-1145 |
| 6 | DIRECTOR<br>ATTN AMSRL MA P<br>L JOHNSON<br>B HALPIN<br>T CHOU<br>AMSRL MA PA<br>D GRANVILLE<br>W HASKELL<br>AMSRL MA MA G HAGNAUER<br>US ARMY RESEARCH LAB<br>ARSNL STREET<br>WATERTOWN MA 02172-0001 |
| 4 | COMMANDER<br>ATTN SMCAR FSE<br>T GORA<br>E ANDRICOPOULOS<br>B KNUTELSKY<br>A GRAF<br>US ARMY ARDEC<br>PCTNY ARSNL NJ 07806-5000 |

| NO. OF COPIES | ORGANIZATION |
|---|---|
| 3 | COMMANDER<br>ATTN SMCAR TD<br>R PRICE<br>V LINDER<br>T DAVIDSON<br>US ARMY ARDEC<br>PCTNY ARSNL NJ 07806-5000 |
| 1 | COMMANDER<br>ATTN F MCLAUGHLIN<br>US ARMY ARDEC<br>PCTNY ARSNL NJ 07806-5000 |
| 5 | COMMANDER<br>ATTN SMCAR CCH T<br>S MUSALLI<br>P CHRISTIAN<br>K FEHSAL<br>N KRASNOW<br>R CARR<br>US ARMY ARDEC<br>PCTNY ARSNL NJ 07806-5000 |
| 1 | COMMANDER<br>ATTN SMCAR CCH V E FENNELL<br>US ARMY ARDEC<br>PCTNY ARSNL NJ 07806-5000 |
| 1 | COMMANDER<br>ATTN SMCAR CCH J DELORENZO<br>US ARMY ARDEC<br>PCTNY ARSNL NJ 07806-5000 |
| 2 | COMMANDER<br>ATTN SMCAR CC<br>J HEDDERICH<br>COL SINCLAIR<br>US ARMY ARDEC<br>PCTNY ARSNL NJ 07806-5000 |
| 1 | COMMANDER<br>ATTN SMCAR CCH P J LUTZ<br>US ARMY ARDEC<br>PCTNY ARSNL NJ 07806-5000 |
| 2 | COMMANDER<br>ATTN SMCAR FSA M<br>D DEMELLA<br>F DIORIO<br>US ARMY ARDEC<br>PCTNY ARSNL NJ 07806-5000 |

| NO. OF COPIES | ORGANIZATION | NO. OF COPIES | ORGANIZATION |
|---|---|---|---|
| 1 | COMMANDER<br>ATTN SMCAR FSA C SPINELLI<br>US ARMY ARDEC<br>PCTNY ARSNL NJ 07806-5000 | 1 | DIRECTOR<br>ATTN P DUTTA<br>US ARMY CRREL<br>72 LYME ROAD<br>HANOVER NH 03755 |
| 11 | DIRECTOR<br>ATTN SMCAR CCB<br>C KITCHENS<br>J KEANE<br>T ALLEN<br>J VASILAKIS<br>G FRIAR<br>T SIMKINS<br>V MONTVORI<br>J WRZOCHALSKI<br>G D'ANDREA<br>R HASENBEIN<br>SMCAR CCB R S SOPOK<br>BENET LABORATORIES<br>WATERVLIET NY 12189-4050 | 1 | DIRECTOR<br>ATTN AMSRL WT L D WOODBURY<br>US ARMY RESEARCH LABORATORY<br>2800 POWDER MILL ROAD<br>ADELPHI MD 20783-1145 |
| | | 2 | DIRECTOR<br>ATTN AMSRL MA P C WHITE<br>J MCLAUGHLIN<br>WATERTOWN MA 02172-0001 |
| 1 | COMMANDER<br>ATTN SMCWV QAE Q C HOWD<br>BLDG 44<br>WATERVLIET ARSENAL<br>WATERVLIET NY 12189-4050 | 4 | COMMANDER<br>ATTN AMSMI RD W MCCORKLE<br>AMSMI RD ST P DOYLE<br>AMSMI RD ST CN T VANDIVER<br>AMSMI RD ST WF M COLE<br>US ARMY MISSILE COMMAND<br>REDSTONE ARSNL AL 35898-5247 |
| 1 | COMMANDER WATERVLIET ARSNL<br>ATTN SMCWV SPM T MCCLOSKEY<br>BLDG 25 3<br>WATERVLIET ARSENAL<br>WATERVLIET NY 12189-4050 | 2 | DIR MATH & COMPUTER SCIENCES DIV<br>ATTN ANDREW CROWSON<br>J CHANDRA<br>US ARMY RESEARCH OFFICE<br>PO BOX 12211<br>RSRH TRI PK NC 27709-2211 |
| 1 | COMMANDER<br>ATTN SMCWV QA QS K INSCO<br>WATERVLIET ARSENAL<br>WATERVLIET NY 12189-4050 | 2 | ENGINEERING SCIENCES DIV<br>ATTN G ANDERSON<br>R SINGLETON<br>US ARMY RESEARCH OFFICE<br>PO BOX 12211<br>RSRH TRI PK NC 27709-2211 |
| 1 | COMMANDER<br>ATTN AMSMC PBM K<br>US ARMY ARDEC<br>PCTNY ARSNL NJ 07806-5000 | 2 | PROJECT MANAGER<br>SADARM<br>PCTNY ARSNL NJ 07806-5000 |
| 1 | COMMANDER<br>ATTN STRBE JBC<br>US ARMY BELVOIR RD&E CTR<br>FORT BELVOIR VA 22060-5606 | 2 | PM TMAS<br>ATTN SFAE AR TMA<br>COL BREGARD<br>C KIMKER<br>PCTNY ARSNL NJ 07806-5000 |

| NO. OF COPIES | ORGANIZATION | NO. OF COPIES | ORGANIZATION |
|---|---|---|---|
| 3 | HERCULES INCORPORATED<br>ATTN G KUEBELER<br>J VERMEYCHUK<br>B MANDERVILLE JR<br>HERCULES PLAZA<br>WILMINGTON DE 19894 | 2 | OLIN CORP<br>FLINCHBAUGH DIV<br>ATTN E STEINER<br>B STEWART<br>PO BOX 127<br>RED LION PA 17356 |
| 1 | CALIFORNIA RESEARCH & TECH<br>ATTN DENNIS ORPHAL<br>5117 JOHNSON DR<br>PLEASANTON CA 94566 | 1 | OLIN CORP<br>ATTN L WHITMORE<br>10101 9TH ST NORTH<br>ST PETERSBURG FL 33702 |
| 1 | IAP RESEARCH INC<br>ATTN A CHALLITA<br>2763 CULVER AVENUE<br>DAYTON OHIO 45429 | 1 | D R KENNEDY AND ASSOC INC<br>ATTN D KENNEDY<br>PO BOX 4003<br>MOUNTAIN VIEW CA 94040 |
| 3 | IAT<br>ATTN T KIEHNE<br>H FAIR<br>P SULLIVAN<br>4030 2 W BRAKER LANE<br>AUSTIN TX 78759 | 1 | LIVERMORE SFTWR TECH CORP<br>ATTN J O HALLQUIST<br>2876 WAVERLY WAY<br>LIVERMORE CA 94550 |
| 1 | SOUTHWEST RSCH INSTITUTE<br>ATTN C ANDERSON<br>6220 CULEBRA RD<br>SAN ANTONIO TX 78284 | 2 | UNIV OF MINNESOTA<br>AHPCRC<br>ATTN G SELL<br>D AUSTIN<br>1100 WASHINGTON AVE S<br>MINNEAPOLIS MN 55415 |
| 1 | INTERFEROMETRICS INC<br>ATTN R LARRIVA VP<br>8150 LESSBURG PIKE<br>VIENNA VA 22100 | 1 | DEFENSE NUCLEAR AGENCY<br>ATTN DR R ROHR<br>INNOVATIVE CONCEPTS DIVISION<br>6801 TELEGRAPH ROAD<br>ALEXANDRIA VA 22310-3398 |
| 2 | KAMAN SCIENCES CORP<br>ATTN D ELDER<br>T HAYDEN<br>PO BOX 7463<br>COLORADO SPRINGS CO 80933 | 1 | EXPEDITIONARY WARFARE DIV N85<br>ATTN DR FRANK SHOUP<br>2000 NAVY PENTAGON<br>WASHINGTON DC 20350-2000 |
| 2 | LORAL VOUGHT SYSTEMS<br>ATTN G JACKSON<br>K COOK<br>1701 W MARSHALL DR<br>GRAND PRAIRIE TX 75051 | 1 | OFFICE OF NAVAL RESEARCH<br>ATTN MR DAVID SIEGEL 351<br>800 N QUINCY ST<br>ARLINGTON VA 22217-5600 |
| 2 | MARTIN MARIETTA CORP<br>ATTN P DEWAR<br>L SPONAR<br>230 EAST GODDARD BLVD<br>KING OF PRUSSIA PA 19406 | 1 | NAVAL SURFACE WARFARE CENTER<br>ATTN JOSEPH H FRANCIS<br>CODE G30<br>DAHLGREN VA 22448 |

1   NAVAL SURFACE WARFARE CENTER
    ATTN JOHN FRAYSSE
    CODE G33
    DAHLGREN VA 22448

1   NOESIS INC
    ATTN ALLEN BOUTZ
    1500 WILSON BLVD STE 1224
    ARLINGTON VA 22209

1   COMMANDER
    ATTN DAVID LIESE
    NAVAL SEA SYSTEMS COMMAND
    2531 JEFFERSON DAVIS HWY
    ARLINGTON VA 22242-5160

1   DEPT OF AEROSPACE ENGNRNG
    ATTN DR ANTHONY J VIZZINI
    UNIVERSITY OF MARYLAND
    COLLEGE PARK MD 20742

1   DEFENSE NUCLEAR AGENCY
    ATTN LTC JYUJI D HEWITT
    INNOVATIVE CONCEPTS DIVISION
    6801 TELEGRAPH RD
    ALEXANDRIA VA 22310-3398

1   NAVAL SURFACE WARFARE CTR
    ATTN MARY E LACY
    CODE D4
    17320 DAHLGREN RD
    DAHLGREN VA 22448-5000


ABERDEEN PROVING GROUND

60  DIR USARL
    ATTN AMSRL CI C MERMEGAN 394
        AMSRL CI C W STUREK 1121
        AMSRL CI CB R KASTE 394
        AMSRL CI S A MARK 309
        AMSRL SL B P DIETZ 328
        AMSRL SL BA J WALBERT 1065
        AMSRL SL BL D BELY 328
        AMSRL SL I D HASKILL 1065
        AMSRL WT P A HORST 390A
        AMSRL WT PA
            T MINOR 390
            C LEVERITT 390
            D KOOKER 390A

    AMSRL WT PB
        E SCHMIDT 120
        P PLOSTINS 120
    AMSRL WT PC R FIFER 390A
    AMSRL WT PD
        B BURNS 390
        W DRYSDALE 390
        K BANNISTER 390
        T BOGETTI 390
        J BENDER 390
        R MURRAY 390
        R KIRKENDALL 390
        T ERLINE 390
        D HOPKINS 390
        C HOPPEL 390
        S WILKERSON 390
        D HENRY 390
        R KASTE 390
        L BURTON 390
        J TZENG 390
    AMSRL WT PD ALC
        A ABRAHAMIAN
        K BARNES
        M BERMAN
        H DAVISON
        A FRYDMAN
        T LI
        W MCINTOSH
        E SZYMANSKI
        H WATKINS
    AMSRL WT T W MORRISON 309
    AMSRL WT TA
        W GILLICH 390
        W BRUCHEY 390
    AMSRL WT TB
        F GREGORY 309
    AMSRL WT TC
        K KIMSEY 309
        R COATES 309
        W DE ROSSET 309
    AMSRL WT TD
        D DIETRICH 309
        G RANDERS PEHRSON 309
        J HUFFINGTON 309
        A DAS GUPTA 309
        J SANTIAGO 309
    AMSRL WT W C MURPHY 120
    AMSRL WT WA
        H ROGERS 394
        B MOORE 394
        A BARAN 394

## USER EVALUATION SHEET/CHANGE OF ADDRESS

This Laboratory undertakes a continuing effort to improve the quality of the reports it publishes. Your comments/answers to the items/questions below will aid us in our efforts.

1. ARL Report Number __ARL-TR-727_____ Date of Report __April 1995_____

2. Date Report Received _____

3. Does this report satisfy a need? (Comment on purpose, related project, or other area of interest for which the report will be used.) _____

_____

_____

4. Specifically, how is the report being used? (Information source, design data, procedure, source of ideas, etc.)

_____

_____

_____

5. Has the information in this report led to any quantitative savings as far as man-hours or dollars saved, operating costs avoided, or efficiencies achieved, etc? If so, please elaborate. _____

_____

_____

6. General Comments. What do you think should be changed to improve future reports? (Indicate changes to organization, technical content, format, etc.) _____

_____

_____

_____

CURRENT
ADDRESS

_____
Organization

_____
Name

_____
Street or P.O. Box No.

_____
City, State, Zip Code

7. If indicating a Change of Address or Address Correction, please provide the Current or Correct address above and the Old or Incorrect address below.

OLD
ADDRESS

_____
Organization

_____
Name

_____
Street or P.O. Box No.

_____
City, State, Zip Code

(Remove this sheet, fold as indicated, tape closed, and mail.)
### (DO NOT STAPLE)

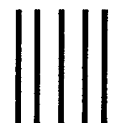**DEPARTMENT OF THE ARMY**

OFFICIAL BUSINESS

# BUSINESS  REPLY MAIL
## FIRST CLASS PERMIT NO 0001, APG, MD

POSTAGE WILL BE PAID BY ADDRESSEE

DIRECTOR
U.S. ARMY RESEARCH LABORATORY
ATTN: AMSRL-WT-PD
ABERDEEN PROVING GROUND, MD 21005-5066